

## Context-Independent, Temperature-Dependent Helical Propensities for Amino Acid Residues

Robert J. Moreau, Christian R. Schubert, Khaled A. Nasr, Marianna Török,  
Justin S. Miller, Robert J. Kennedy, and Daniel S. Kemp\*

Department of Chemistry, Room 6-433, Massachusetts Institute of Technology,  
Cambridge, Massachusetts 02139

Received May 26, 2009; E-mail: kemp@mit.edu

**Abstract:** Assigned from data sets measured in water at 2, 25, and 60 °C containing  $^{13}\text{C}=\text{O}$  NMR chemical shifts and  $[\theta]_{222}$  ellipticities, helical propensities are reported for the 20 genetically coded amino acids, as well as for norvaline and norleucine. These have been introduced by chemical synthesis at central sites within length-optimized, spaced, solubilized  $\text{Ala}_{19}$  hosts. The resulting polyalanine-derived, quantitative propensity sets express for each residue its temperature-dependent but context-independent tendency to forego a coil state and join a preexisting helical conformation. At 2 °C their rank ordering is: P < G < H < C, T, N < S < Y, F, W < V, D < K < Q < I < R, M < L < E < A; at 60 °C the rank becomes: H, P < G < C < R, K < T, Y, F < N, V < S < Q < W, D < I, M < E < A < L. The  $\Delta\Delta G$  values, kcal/mol, relative to alanine, for the cluster T, N, S, Y, F, W, V, D, Q, imply that at 2 °C all are strong breakers:  $\Delta\Delta G_{\text{mean}} = +0.63 \pm 0.11$ , but at 60 °C their breaking tendencies are dramatically attenuated and converge toward the mean:  $\Delta\Delta G_{\text{mean}} = +0.25 \pm 0.07$ . Accurate modeling of helix-rich proteins found in thermophiles, mesophiles, and organisms that flourish near 0 °C thus requires appropriately matched propensity sets. Comparisons are offered between the temperature-dependent propensity assignments of this study and those previously assigned by the Scheraga group; the special problems that attend propensity assignments for charged residues are illustrated by lysine guest data; and comparisons of errors in helicity assignments from shifts and ellipticity data show that the former provide superior precision and accuracy.

### Introduction

Much prior effort has been directed toward quantitative prediction of aqueous helix-coil energetics from peptide and protein residue compositions and sequences.<sup>1–3</sup> These predictions have likely medical relevance.<sup>4</sup> During the folding of many biosynthesized protein sequences, a pivotal early event is the formation of solvent-exposed, weakly stabilized, short helical regions,<sup>5</sup> and their mutation-induced destabilization with resulting mis-folding may be a primary factor in the onset of particular human degenerative diseases.<sup>6</sup> Algorithms that tie helical sequence to energetics can thus provide chemical insight into mutation-based mis-folding, and during the 1990s a widely cited helicity algorithm was introduced.<sup>7</sup>

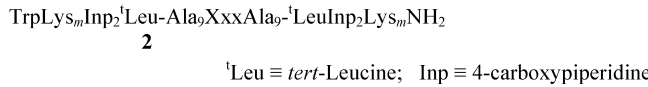
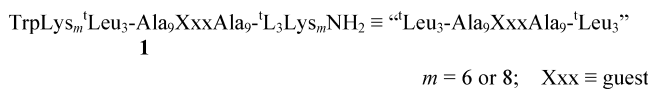
In addition to dependencies of helicity on sequence length and end-region structure, this and related algorithms embody parameters assigned from helicity-modifying single and double guest substitutions within medium-length host peptides. Although these characterized a large inventory of energetic effects,<sup>8</sup> for practical reasons, temperature dependences for these parameters were usually extrapolated from data measured at the low end of the aqueous temperature range (0–10 °C).

Such extrapolations may result in large errors, since the single pertinent host-guest study, carried out over the range of 10–70 °C, reveals temperature dependences that are strongly residue-specific.<sup>9</sup> A need for new temperature-dependent helicity data is also underlined by a remarkable recent observation. Genomic analyses of thermophilic organisms show that seven amino acid residues appear within their protein helices with unusual frequency,<sup>10,11</sup> yet five of these residues are helix breakers at 0 °C, and alanine, the strongest helix former at this temperature,<sup>12</sup> is not included among the seven. We here report a new host-

- (1) Doig, A. J. *Biophys. Chem.* **2002**, *101*–*102*, 281–285.
- (2) Shi, Z.; Olson, C. A.; Bell, A. J., Jr.; Kallenbach, N. R. *Biopolymers* **2001**, *60*, 366–380.
- (3) Maison, W.; Arce, E.; Renold, P.; Kennedy, R. J.; Kemp, D. S. *J. Am. Chem. Soc.* **2001**, *123*, 10245–10254.
- (4) Kelly, J. W. *Curr. Opin. Struct. Biol.* **1998**, *8*, 101–106.
- (5) (a) Baldwin, R. L.; Rose, G. D. *Trends Biochem. Sci.* **1999**, *24*, 77–83. (b) Werner, J. H.; Dyer, H. B.; Fesinmeyer, R. M.; Andersen, N. H. *J. Phys. Chem. B* **2002**, *106*, 487–494.
- (6) (a) Viguera, A. R.; Villegas, V.; Aviles, F. X.; Serrano, L. *Folding Design* **1996**, *2*, 23–33. (b) Pan, K. M.; Baldwin, M.; Nguyen, J.; Gasset, M.; Serban, A.; Groth, D.; Mehlhorn, I.; Hang, Z.; Fletterick, R. J.; Cohen, F. E.; Prusiner, S. B. *Proc. Natl. Acad. Sci. U.S.A.* **1993**, *90*, 10962–10966.
- (7) (a) Lacroix, E.; Viguera, A. R.; Serrano, L. *J. Mol. Biol.* **1998**, *284*, 173–192. (b) Muñoz, V.; Serrano, L. *J. Mol. Biol.* **1995**, *245*, 297–308.
- (8) Muñoz, V.; Serrano, L. *Biopolymers* **1997**, *41*, 495–509.
- (9) (a) Wójcik, J.; Altmann, K.-H.; Scheraga, H. A. *Biopolymers* **1990**, *30*, 121–134. (b) Scheraga, H. A. *Perspectives in Structural Biology*; Vijayan, M., Yathindra, N., Kolaskar, A. S., Eds.; Indian Academy of Sciences: Bangalore, 1999; pp 275–292. (c) Scheraga, H. A.; Vila, J. A.; Ripoli, D. R. *Biophys. Chem.* **2002**, *101*–*102*, 255–265.
- (10) Chakrabarty, S.; Varadarajan, R. *Biochemistry* **2002**, *41*, 8152–8161.
- (11) Zeldovich, K. B.; Berezovsky, I. N.; Shakhnovich, E. I. *PLoS Comput. Biol.* **2007**, *3*, 62–72.
- (12) Rohl, C. A.; Chakrabarty, A.; Baldwin, R. L. *Protein Sci.* **1995**, *5*, 2623–2637.

guest study, designed to meet stringent accuracy requirements and carried out over a large temperature range.<sup>13</sup>

A useful host must be experimentally tractable, and it must retain detectable helicity over most of the aqueous temperature range. Among homopeptides, a polyalanine core region  $\text{Ala}_n$ ,  $12 \leq n \leq 45$  meets the first condition if it is N- and C-linked through spacing elements to solubilizing, aggregation-inhibiting polylysine caps.<sup>14</sup> In a series of foundation studies, we have previously calibrated host helicity assignments from both circular dichroism ellipticities  $[\theta]_{222}$ <sup>15</sup> and  $^{13}\text{C}=\text{O}$  NMR chemical shifts<sup>16</sup> and reported a definitive set of length- and temperature-dependent values for the alanine helical propensity  $w_{\text{Ala}}[n,T]$ .<sup>13,17</sup> We have also demonstrated that propensity assignment accuracies are optimized by the 19-residue lengths of chemically synthesized mutants **1**, helically characterized by chemical shifts,<sup>13</sup> and mutants **2**, helically characterized by ellipticities.<sup>15</sup>



$$[\theta]_{222,\text{Exper},n,T} = \text{FH}[\theta]_{222,\text{H},n,T} + (I - \text{FH})[\theta]_{222,\text{C},n,T} \cong \text{FH}[\theta]_{222,\text{H},n,T} \quad (1)$$

$$[\theta]_{222,\text{H},n,T} = [\theta]_{222,\text{H},\infty,T}(I - X/n) \quad 0 \leq X \leq 1.0 \quad (2)$$

This report consummates these efforts. It assigns temperature-dependent helical propensities for the 20 genetically coded amino acid residues and for selected others. It then correlates these with the classic benchmarks reported by the Scheraga group.<sup>9</sup>

The properties of polyalanine hosts ensure that new modeling opportunities can follow from these assignments. For any helical sequence, the set of its propensities embodies helicity contributions that result solely from residue composition, and a second set characterizes context effects that embody helicity perturbations attributable to the sequence order. A polyalanine-derived propensity set combined with a compatible context set would uniquely allow chemically based structural modeling of the fundamental energetics of helix formation. In the following section we define basic concepts that are developed in the

- (13) Nasr, K. A.; Schubert, C. R.; Török, M.; Kennedy, R. J.; Kemp, D. S. *Biopolymers* **2009**, *91*, 311–320.
- (14) (a) Kemp, D. S.; Curran, T. C.; Boyd, J. G.; Allen, T. A. *J. Org. Chem.* **1991**, *56*, 6683–6697. (b) Kemp, D. S.; Allen, T. A.; Oslock, S. L. *J. Am. Chem. Soc.* **1995**, *117*, 6641–6657. (c) Kemp, D. S.; Allen, T. A.; Oslock, S. L.; Boyd, J. G. *J. Am. Chem. Soc.* **1996**, *118*, 4240–4248. (d) Kemp, D. S.; Oslock, S. L.; Allen, T. A. *J. Am. Chem. Soc.* **1996**, *118*, 4249–4255. (e) Cammers-Goodwin, A.; Allen, T. A.; Oslock, S. L.; McClure, K. F.; Lee, J. H.; Kemp, D. S. *J. Am. Chem. Soc.* **1996**, *118*, 3082–3090. (f) Miller, J. S.; Kennedy, R. J.; Kemp, D. S. *Biochemistry* **2001**, *40*, 305–309. (g) Kennedy, R. J.; Tsang, K.-Y.; Kemp, D. S. *J. Am. Chem. Soc.* **2002**, *124*, 934–944. (h) Miller, J. S.; Kennedy, R. J.; Kemp, D. S. *J. Am. Chem. Soc.* **2002**, *124*, 945–962.
- (15) Job, G. E.; Kennedy, R. S.; Heitmann, B.; Miller, J. S.; Walker, S. M.; Kemp, D. S. *J. Am. Chem. Soc.* **2006**, *128*, 8227–8233.
- (16) Kennedy, R. J.; Walker, S. M.; Kemp, D. S. *J. Am. Chem. Soc.* **2005**, *127*, 16961–16968.
- (17) Details concerning these assignments appear in the Supporting Information of ref 13.

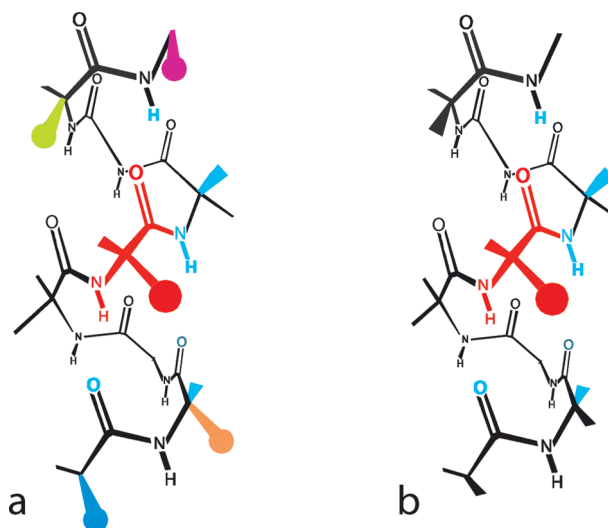


**Figure 1.** Contacts of a red guest residue at a mutant site  $i$  within a typical  $\alpha$ -helix (a) and within an idealized  $\alpha$ -helix in which local context effects are minimal (b). In (a), the red guest atoms contact the cyan neighboring backbone as well as side chain atoms of residues at  $(i \pm 3)$  and  $(i \pm 4)$  separations (green, magenta, orange, and blue circles). Both helical propensities and context effects are required to characterize the energetics of these interactions. For case (b), the contacts between side chains are minimal, and only the cyan contacts perturb helicity significantly. Their sequence-independent energetics are defined by the helical propensities.

discussion and also raise a practical issue. How accurate are propensity values that are solely assigned from CD ellipticities measured for mutants **2**?

**Helical Propensities and Context Effects.** Based on the hypothesis that local effects control helical stability, most helicity algorithms are built from two sets of parameters. The first contains the 20 quantitative helical propensities, each reflecting for a particular residue, its temperature-dependent equilibration between coil and  $\alpha$ -helical states. A much larger second set consists of temperature-dependent energetic corrections for paired charge, polar, and hydrophobic interactions between a guest side chain and those of its four neighbors, Figure 1a. The contribution to global helicity from helical propensities thus reflects residue composition, and the contribution from the set of context parameters embodies sequence dependence.<sup>2,18,19</sup>

Standard modeling tools of molecular chemistry should, at least in principle, be applicable to any helical sequence to predict its temperature-dependent helix–coil energetics in water. In fact, model validation has been plagued by doubts concerning the reliability of available helical propensity sets, many of which have been challenged as incorporating hidden host-dependent biases. The polyalanine regions of mutants **1** and **2** can resolve this imbroglio, since it is generally agreed that a helical context that consists solely of alanine side chains, with their minimal hydrophobic bulk and absence of charge or polarity, provides the closest experimental approximation to the modeler's context-free  $\alpha$ -helix of Figure 1b.<sup>20</sup>

**Background.** The polyalanine mutants **1** and **2** have a second essential feature. We have previously tailored their lengths to

- (18) Zerkowski, J. A.; Powers, E. T.; Kemp, D. S. *J. Am. Chem. Soc.* **1997**, *119*, 1153–1154.
- (19) Kallenbach, N. R.; Spek, E. J. *Methods Enzymol.* **1998**, *295*, 26–41.
- (20) (a) Padmanabhan, S.; York, E. J.; Gera, L.; Stewart, J. M.; Ridgeway, T.; Baldwin, R. L. *Biochemistry* **1994**, *33*, 8604–8609. (b) Creamer, T. P.; Rose, G. D. *Protein Sci.* **1995**, *4*, 1305–1314.

maximize sensitivity to guest substitution,<sup>13</sup> and alone among the medium length uncharged homopeptide hosts that can be constructed from the natural amino acids, they can retain helicity over a maximal temperature range. Only the oligopeptide mutants synthesized and studied by the Scheraga group have been optimized in this manner.<sup>9</sup> As an introduction to the data sections that follow, we compare and contrast these two design strategies.

Studies carried out in the 1970s defined the experimental foundations for all subsequent quantitative studies of peptide helicity. The  $\alpha$ -helices formed by polylysine or polyglutamate oligopeptides allowed the first experimental characterization of the highly cooperative temperature- and length-dependent helicities that characterize isolated peptides solvated by water. The data were inconsistent with simple all-or-none helix-coil energetic models, but good fits resulted from two-parameter algorithms, based on statistical mechanical ensembles of equilibrated nonhelical, completely helical, and partially helical conformations.<sup>21</sup> In these algorithms, cooperativity is attributed to an energetically unfavorable helix initiation step that is followed by a series of helix propagation steps. In each of these, the marginally favorable helical weight of a single new residue is added to the weight of the previous helical sequence for each ensemble conformation.

The resulting overall ensemble weighting ensures that if a peptide or oligopeptide that lacks tertiary packing exhibits detectable helicity, it will melt reversibly and progressively over a broad temperature region. A small temperature increment corresponds to a correspondingly small degree of melting, reflecting a proportionate increase in the relative abundance of conformations that contain shorter helices.

In the widely used Lifson-Roig algorithm,<sup>22</sup> propagation is modeled by a temperature- and residue-dependent parameter  $w$ , the helical propensity, which is an equilibrium constant that defines the incremental helicity change for a sequence if its length is increased by one residue. For helix-breakers,  $w$  values lie in the range 0–1.0, but for helix-formers,  $w$  usually lies between 1.0 and 1.8.

The overall helicity contribution from propagation for any helical region is proportional to the product of the  $w$  values of its residues, and their mean magnitude within a sequence defines the minimal length required for it to exhibit detectable helicity. If this mean lies between 1.0 and 1.1, a detectably helical sequence must contain more than a hundred residues, but a peptide of moderate length can be detectably helical if the mean  $w$  value exceeds 1.3.

Prior to 1989, when Marqusee, Robbins, and Baldwin reported that short peptides are highly helical if they are alanine-rich,<sup>23</sup> oligopeptides were the sole mutant options, and consistent with a prior study,<sup>24</sup> in 1971 Scheraga and co-workers reported a pair of helical oligopeptides constructed from covalently modified glutamines that met the stringent needs of a breakthrough host-guest helicity study, designed to be conducted in water over a broad temperature range.<sup>25</sup>

- (21) Poland, D.; Scheraga, H. A. *Statistical Mechanical Theory of Order-Disorder Transitions in Biological Macromolecules*; Academic Press: New York, 1970.
- (22) (a) Lifson, S.; Roig, A. *J. Chem. Phys.* **1961**, *34*, 1963–1974. (b) Qian, H.; Schellman, J. A. *J. Phys. Chem.* **1992**, *96*, 3987–3994. (c) Kemp, D. S. *Helv. Chim. Acta* **2002**, *35*, 4392–4423.
- (23) Marqusee, S.; Robbins, V. H.; Baldwin, R. L. *Proc. Natl. Acad. Sci. U.S.A.* **1989**, *86*, 5286–5290.
- (24) Lotan, N.; Yarov, A.; Berger, A. *Biopolymers* **1966**, *4*, 365–368.

The large perturbing effects of guests on melting curves posed a design challenge that was solved by use of a pair of hosts, derived from structurally similar helix-forming residues. Substitutions by helix formers within the less helical host, formed from N<sup>5</sup>-(3-hydroxypropyl-L-glutamine), yielded mutants with a planned melting range 10–70 °C, and this range was shared by mutants derived from helix breakers, incorporated within a more helical host formed from N<sup>5</sup>-(4-hydroxybutyl-L-glutamine). Analysis of the resulting mutant data yielded the first set of temperature dependent helical propensities for the natural amino acids. Ten of these decreased monotonically with increasing temperature, five exhibited curved temperature dependences with maxima within the range of 15–40 °C, and the remaining five increased monotonically with increasing temperature. Within the latter group, the  $\beta$ -branched hydrophobic residue valine, a helix breaker near 0 °C, becomes a weak helix former at higher temperatures, a property confirmed from a study of helical polyvalines.<sup>26</sup> The helical propensity of alanine ranked it sixth in the list of helix formers, a value that decreased within the range 0–60 °C from 1.1 to 1.0, but very different values were reported in the 1990s for alanine residues of alanine-rich peptides of medium length that were solubilized by spaced polar or charged residues and studied at or near 0 °C.<sup>27</sup> In these reports, alanine was ranked as the strongest helix former, with a  $w_{\text{Ala}}$  between 1.5 and 1.8. These assignments were initially questioned, and alternatives were offered that attributed the high helicities of these peptides to context-dependent helix-stabilizing effects of glutamine and lysine residues.<sup>28</sup> Subsequent guest mutations within other hosts supported the new alanine rank order,<sup>29</sup> and later low temperature assignments of  $w_{\text{Ala}}$  within polyalanines of adequate length confirmed it.<sup>14g,h,30</sup>

To lay a foundation for the present study, we characterized  $w_{\text{Ala}}[n,T]$  values for central residue contexts of 'Leu-Ala<sub>n</sub>'-Leu,  $n = 9$  to 23, in water between 2 and 80 °C, using <sup>13</sup>C=O NMR chemical shifts of the alanine backbone amides as helicity monitors. The following assignments for  $w_{\text{Ala}}[19,T]$  resulted: 2 °C, 1.56; 10 °C, 1.52; 25 °C, 1.39; 37 °C, 1.30; 52 °C, 1.22; 60 °C, 1.17; 80 °C, 1.11.<sup>13,17</sup> Rather than using a pair of hosts for mutation studies over the temperature range of 2 to 80 °C, we tailored the polyalanine host length to provide an optimal trade-off between the helicity properties of mutants derived from guests that are strong helix-breakers as well as those that are strong helix-formers. For breaking guests, the mutant length must be sufficiently long to retain characterizable helicity within the range 60 to 80 °C; for forming guests, the mutant length must be sufficiently short to allow characterization of the helicity

- (25) Von Dreele, P. H.; Lotan, N.; Ananthanarayanan, V. S.; Andreatta, R. H.; Poland, D.; Scheraga, H. A. *Macromolecules* **1971**, *4*, 408–417.
- (26) Gô, M.; Hesselink, F. T.; Gô, N.; Scheraga, H. A. *Macromolecules* **1974**, *7*, 459–467.
- (27) (a) Padmanabhan, S.; Marqusee, S.; Ridgeway, T.; Laue, T. M.; Baldwin, R. L. *Nature* **1990**, *344*, 268–270. (b) Park, S. H.; Shalongo, W.; Stellwagen, E. *Biochemistry* **1993**, *32*, 7048–7053. (c) Chakrabarty, A.; Korteme, T.; Baldwin, R. L. *Protein Sci.* **1994**, *3*, 843–852. (d) Rohl, C. A.; Chakrabarty, A.; Baldwin, R. L. *Protein Sci.* **1994**, *5*, 2623–2637.
- (28) (a) Vila, J.; Williams, R. L.; Grant, J. A.; Wójcik, J.; Scheraga, H. A. *Proc. Natl. Acad. Sci. U.S.A.* **1992**, *89*, 7821–7825. (b) Williams, L.; Kather, K.; Kemp, D. S. *J. Am. Chem. Soc.* **1998**, *120*, 11033–11043.
- (29) (a) Lyu, P. C.; Liff, M. I.; Marky, L. A.; Kallenbach, N. R. *Science* **1990**, *250*, 669–673. (b) O'Neil, K. T.; DeGrado, W. F. *Science* **1990**, *250*, 646–650. (c) Blaber, M.; Zhang, X.-J.; Lindstrom, J. D.; Pepiot, S. D.; Baase, W. A.; Matthews, B. W. *J. Mol. Biol.* **1994**, *235*, 600–624.
- (30) Kennedy, R. J. Ph. D. Thesis, Massachusetts Institute of Technology: Cambridge, MA, 2004.

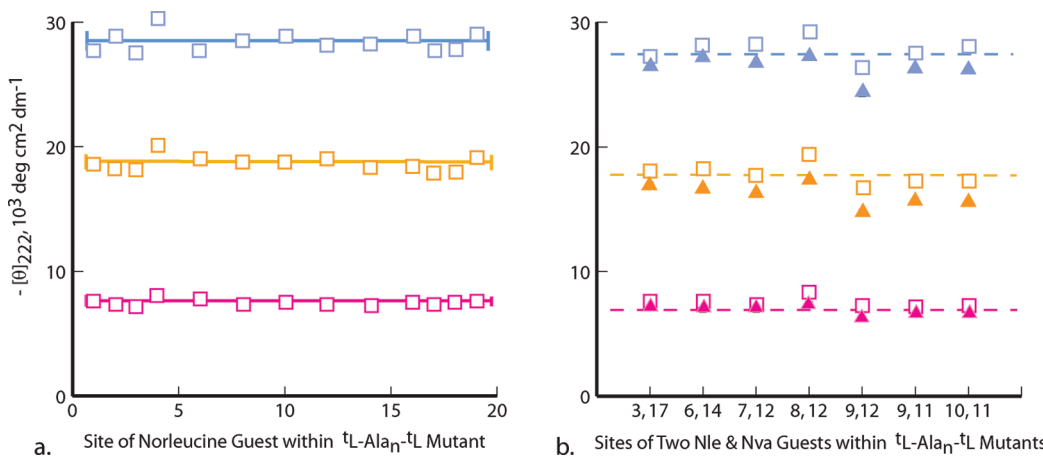


**Figure 2.** (a) Values of  $[\theta]_{222}$  for specifically sited single Nle  $\equiv$  norleucine guests within the 'Leu-Ala<sub>19</sub>'-Leu host at 2 °C (blue), 25 °C (orange), and 60 °C (magenta). The solid lines correspond to mean values of  $[\theta]_{222}$ . (b) Values of  $[\theta]_{222}$  for spaced pairs of Nle (□) and Nva norvaline guests (▲) within the series 2 Ala<sub>19</sub> host at 2 °C (blue), 25 °C (orange), and 60 °C (magenta). The dotted lines correspond to  $[\theta]_{222}$  values for this host.

difference between mutant and host within the range 2–10 °C. Modeling was initially used to select an optimal mutant length of nineteen residues, and this choice was then validated empirically for mutants **1**.<sup>13</sup> The strong helix-former norvaline and the pair of strong helix breakers glycine and proline were selected as guests, since their propensities were expected to bracket those for the natural residues. For these mutants <sup>13</sup>C=O NMR shift data were measured within 2–80 °C, and  $w_{\text{Gly}}$ ,  $w_{\text{Pro}}$ , and  $w_{\text{Nva}}$  were assigned with acceptable precision. Values for  $w_{\text{Nva}}$  closely resemble those for  $w_{\text{Ala}}$ , decreasing comparably with increasing temperature, but values for  $w_{\text{Gly}}$  and  $w_{\text{Pro}}$  increase significantly, suggesting that sequences of helical proteins found in mesophiles or thermophiles can include these residues with a reduced folding penalty. Comparisons of the sets of temperature dependent propensities assigned by the Scheraga group and those from the present study are explored in the discussion section.

**Precision for Circular Dichroism Ellipticities at 222 nm,  $[\theta]_{222}$ , Measured for Mutants 2.** Nearly universally regarded as the “gold standard” for quantitative helicity assignments, the experimental per-residue molar ellipticities  $[\theta]_{222,\text{Exper},n,T}$  allow calculation of fractional helicities FH, defined as the mole fraction of helical residues within a partially helical sequence, eqs 1 and 2. The intensity of the helical CD chromophore at 222 nm, together with the minimal intensity of chromophores at that wavelength for all other peptide backbone conformations, justifies a frequently applied approximation that disregards the coil term  $[\theta]_{222,\text{C},n,T}$ , as seen in eq 3. The  $[\theta]_{222,\text{Exper},n,T}$  data for mutants **2** are corrected by subtraction of the minor contributions of N- and C-caps,<sup>14f,h,15</sup> and FH values are then assigned from host-assigned  $[\theta]_{222,\text{H},n,T}$  and  $[\theta]_{222,\text{C},n,T}$ .<sup>31</sup>

$$\text{FH} = ([\theta]_{222,\text{Exper},n,T} - [\theta]_{222,\text{C},n,T}) / ([\theta]_{222,\text{H},n,T} - [\theta]_{222,\text{C},n,T}) \cong [\theta]_{222,\text{Exper},n,T} / [\theta]_{222,\text{H},n,T} \quad (3)$$

To assign precisions for  $[\theta]_{222,\text{Exper},n,T}$ , we carried out nineteen (Ala  $\rightarrow$  Nle) single residue replacements within the series **2** host peptide, giving the  $T$ -dependent ellipticities of Figure 2a. Two motivations governed selection of the norleucine Nle residue for this assignment. At the three temperatures of this study, Nle is a slightly stronger helix former than alanine<sup>32</sup>

(compare the solid lines of Figure 2a with the broken lines of Figure 2b), which ensures that the mutant ellipticity signal at 60 °C remains sufficiently intense to be interpretable. Moreover, lysine and norleucine share a carbon skeleton, providing useful comparisons for lysine data, as discussed in a later section.

Convincing site dependences are not detectable within the Figure 2a data set, and treated as randomly distributed, ellipticities at all temperatures have standard deviations of 3 to 4% of the average value. Padmanabhan et al. reported similar values at 0 °C for alanine-rich peptides,<sup>20a</sup> and in studies of the length dependence of  $[\theta]_{222,\text{Exper}}$  for a series **2** capped Ala<sub>n</sub> series,  $12 \leq n \leq 20$ , we assigned respective relative measurement precisions for  $[\theta]_{222,\text{Exper},n,T}$  at 2, 25, and 60 °C of 4, 5, and ca. 10%.<sup>14f</sup> The higher latter value can be attributed to the weak high-temperature CD intensities typical of short helical peptides ( $n < 17$ ).

The data of Figure 2b illustrate an important consequence. Two sets of seven  $[\theta]_{222}$  measurements are shown for mutants that incorporate pairs of contiguous or spaced norleucine and norvaline guests. A comparison with Figure 1a shows that the residue pairs at (9, 12) and (8, 12) spacings may have ( $i, i + 3$ ) and ( $i, i + 4$ ) side chain contacts, with resulting helicity perturbations. The mutants that contain ( $i, i + 4$ ) guest pairs have slightly larger than average  $[\theta]_{222}$  values, and those that contain ( $i, i + 3$ ) guest pairs have slightly smaller values, but both lie within measurement error, and neither can be used to verify or refute the existence of the corresponding helicity changes. Thus  $[\theta]_{222}$  measurements lack the precision required for assignments of small context-dependent helicity perturbations. In the next two sections, we explore the key issues of methodological precision and accuracy, preconditions for any rigorous discussion of propensity values.

**Precisions of <sup>13</sup>C=O NMR Chemical Shift Measurements for Alanine Residues; T-Dependent Shift Scans for the Spaced, Solubilized Series 1 Ala<sub>19</sub> Host and for its Single-Site Mutants; Accuracies of Shift-derived FH<sub>i</sub>.** The filled circles of Figure 3a provide complete <sup>13</sup>C=O NMR chemical shift scans measured in water at 2, 25, and 60 °C for alanine residues of the host. Also shown are analogous mutant **1** alanine site scans for guests: Leu, Ile, Nle, Nva, and Val. The error calculated from repeated measurements is  $\pm 0.02$  ppm; implying that the shift precision, defined relative to the shift range, exceeds that assigned in the preceding section for  $[\theta]_{222}$  values.

(31) Heitmann, B.; Job, G. E.; Kennedy, R. S.; Miller, J. S.; Walker, S. M.; Kemp, D. S. *J. Am. Chem. Soc.* **2005**, 127, 1690–1704.

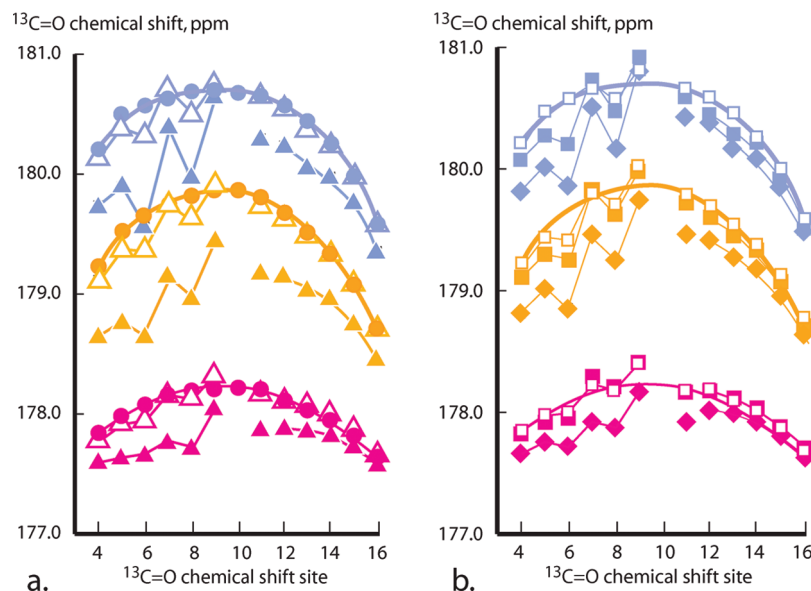


**Figure 3.** Values of  $^{13}\text{C}=\text{O}$  NMR chemical shifts in water at 2 °C (blue), 25 °C (orange), 60 °C (magenta). Host values, ●. Values for mutants **1** 'Leu-Ala<sub>9</sub>XxxAla<sub>9</sub>'Leu are coded as follows: (a) △: Xxx = Nva; ▲: Xxx = Val. (b) ■: Xxx = Nle; □: Xxx = Leu; ♦: Xxx = Ile. The closed-line fits to host data that appear in a are repeated in b. Each shift is site-coded within each peptide by a specific  $^{13}\text{C}/^{12}\text{C}$  ratio.

The NMR chemical shift of a specific backbone  $^{13}\text{C}=\text{O}$  nucleus reflects a weighted average of contributions from local magnetic anisotropies. These are residue-specific and sensitive to changes in neighboring structure and local solvation, but the helix–coil conformational anisotropy difference almost invariably dominates, allowing accurate identification of helical regions within globular proteins as well as assignment of fractional site helicities  $\text{FH}_i$  for peptides.<sup>33,34</sup>

Except at end regions, the host shift scans of Figure 3a define smooth envelopes with maximal values near the sequence center. This is the signature of averages over equilibrated ensemble conformations, of which more than 60% contribute to experimental shifts at central sites, but only 11% contribute at end sites.<sup>13,17</sup> The environment of backbone atoms near end regions cause their shifts to deviate significantly from envelope extrapolations. Pertinent anisotropies include atypical solvent exposure and proximity to the terminal helix dipoles and to spacer side chains.

End region shift issues also arise for partially helical conformations within the ensemble, whose abundance-weighted averages define the experimental shifts. For maximal  $\text{FH}_i$  assignment accuracy, we modify the standard two-state helix–coil model by assigning experimentally derived weights to conformations with helical regions that start or stop at each site *i*. Both  $\text{FH}_i$ , eq 4, and modeled chemical shifts  $\delta^{13}\text{C}=\text{O}_{i,\text{Exp}}$ , eq 5, are thus written as sums of weights for conformations that are initiated (I), terminated (T), or continued (C) at that site. The required four temperature-dependent calibration constants of eq 5 have been previously characterized.<sup>17</sup>

$$\text{FH}_i = \text{FH}_{i,I} + \text{FH}_{i,C} + \text{FH}_{i,T} \quad (4)$$

$$\begin{aligned} \delta^{13}\text{C}=\text{O}_{i,\text{Exp}} = & \text{FH}_{i,I} \delta^{13}\text{C}=\text{O}_{\text{Hel},I} + \text{FH}_{i,C} \delta^{13}\text{C}=\text{O}_{\text{Hel},C} + \\ & \text{FH}_{i,T} \delta^{13}\text{C}=\text{O}_{\text{Hel},T} + (1 - \text{FH}_i) \delta^{13}\text{C}=\text{O}_{\text{Coil}} \end{aligned} \quad (5)$$

What perturbations are expected for alanine  $^{13}\text{C}=\text{O}$  chemical shifts if a guest side chain replaces an alanine methyl at site 10? The mutant data of Figures 3ab show that large fluctuations in shift magnitude appear at sites 6 to 9, which lie N-terminal

to the guest. These are plausibly attributable to local shift anisotropies attributable to side chain contacts, guest-induced distortions in backbone angles that maintain helical structure, and local solvent shielding. Perturbations C-terminal to the guest are small and almost invariably lie within measurement error. The  $^{13}\text{C}=\text{O}$  chemical shifts thus offer a unique advantage as helicity reporting tools, provided their accuracy is maximized by introducing  $^{13}\text{C}$ -labels solely within alanine regions characterized by smooth shift envelopes.<sup>13</sup> We usually rely on central sites within the Ala<sub>9</sub> C-terminal region.

To test reporting fidelity for these sites, we correlated two 21-guest sets of shifts, measured at alanine sites 14 and 15. The filled squares of Figure 4 depict the results. Within measurement error, identical shift rank orders are seen, with the following correlation coefficients and standard deviations, 2 °C, 0.997, 0.03 ppm; 25 °C, 0.997, 0.02 ppm; 60 °C, 0.98, 0.02 ppm. These values confirm the expected  $\text{FH}_i$  precision and accuracy.

An analogous optimization of measurement sites is unavailable if  $[\theta]_{222}$  ellipticities replace shifts as quantitative helicity monitors. Both  $\text{FH}$  and  $[\theta]_{222}$  are global averages for entire helical regions, and for series **2** mutants, the  $[\theta]_{222}$  values and  $\text{FH}$  assignments invariably include potentially anomalous contributions from guests and their neighboring alanines. The accuracy of Equation 3, used to calculate  $\text{FH}$  from  $[\theta]_{222}$  data, thus rests on the accuracy of its calibration constant  $[\theta]_{222,\text{H},n,T}$ , which is necessarily assigned from host helicity data. In the Supporting Information we show that for specific guests, use of host-derived values for  $[\theta]_{222,\text{H},n,T}$  underestimates mutant  $\text{FH}$ .<sup>35</sup>

From modeled data we have previously shown that over the range of possible guests, shifts and  $[\theta]_{222}$  values correlate strictly

- (32) (a) Padmanabhan, S.; Baldwin, R. L. *J. Mol. Biol.* **1991**, 219, 135–137. (b) Lyu, P. C.; Sherman, J. C.; Chen, A.; Kallenbach, N. R. *Proc. Natl. Acad. Sci. U.S.A.* **1991**, 88, 5317–5326.
- (33) Wishart, D. S.; Richards, F. M.; Sykes, B. D. *J. Mol. Biol.* **1991**, 222, 311–333.
- (34) Wishart, D. S.; Sykes, B. D. *Methods Enzymol.* **1994**, 239, 363–392.
- (35) As detailed in the Supporting Information, evidence includes a 203 nm test as well as quantitative bounds on required corrections to  $[\eta]_{222,\text{H},n,T}$ .

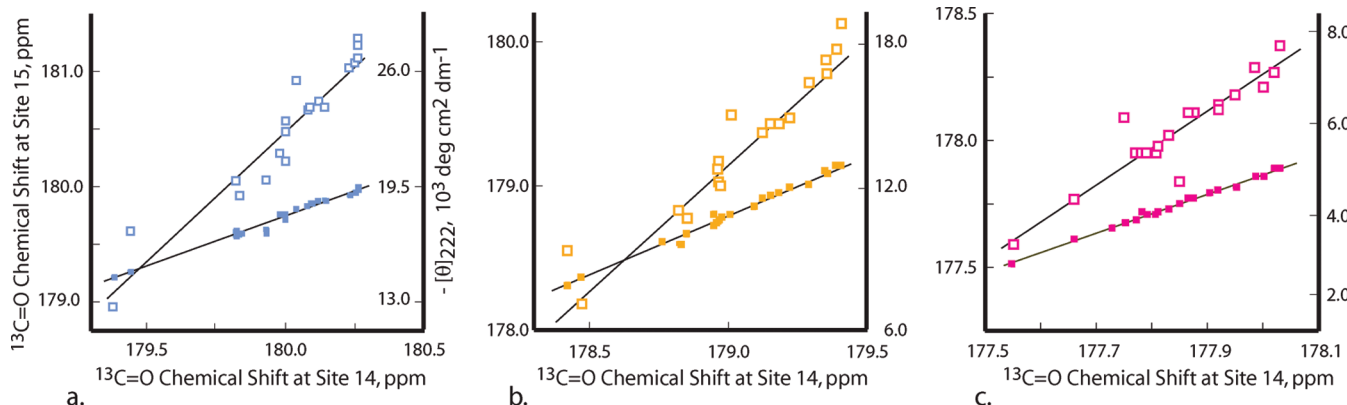


**Figure 4.** Shift regressions measured in water at neutral pH. Temperatures: (a) 2 °C (blue), (b) 25 °C (orange), (c) 60 °C (magenta). Mutants containing aspartate, glutamate, and histidine were studied at pH 7;  $[\theta]_{222}$  values for Cys and Trp mutants were not measured; Pro data are omitted for clarity since they fall far to the left of depicted graph sites. ■ correlate  $^{13}\text{C}$ =O chemical shifts at sites 15 and 14 for 21 series **1** mutants, and lines depict linear regressions. □ correlate  $[\theta]_{222}$  data measured in mutants **2** with selected site 14 shift data. Mean rank orders for shift data appear below, with black vertical lines that distinguish helix breakers from formers: 2 °C: P < G < H < C, T, N < S < Y, F, W < V, D < K < Q < I < R, M < L < E < Nva, Nle < A 25 °C: P < H, G < C, T < N < S, Y, F < D, V < K < W < Q < R < I < M < L < E < Nva, A 60 °C: H, P < G < C < R, K < T, Y, F < N, V < S < Q < W, D < I, M < E < Nva < A < L, Nle.

**Table 1.** T-Dependent Linear Regression Slopes and Intercepts with Standard Deviations and Correlation Coefficients for the Pair of  $w_{\text{XXX}}/w_{\text{Ala}}$  Sets Assigned from  $[\theta]_{222}$  Values of Mutants **2** and  $^{13}\text{C}$ =O NMR Chemical Shifts at Site 14 of Mutants **1**.<sup>a</sup> See Figure 5 Correlations

T, °C	slope	intercept	fit (SD)	CC	mean Δ, %
2	1.06	-0.15	0.10	0.95	+30
25	1.07	-0.10	0.08	0.96	+18
60	1.00	+0.07	0.09	0.92	-11

<sup>a</sup> Mean Δ are Percentage Differences for Shift- vs.  $[\theta]_{222}$ -Derived  $w_{\text{XXX}}/w_{\text{Ala}}$ : XXX = Nle, Nva, A, E, L, K, M, I, Q, R, D, V, F, Y, S, N, T, G, P.

linearly.<sup>13</sup> The open squares of Figure 4 test the quality of this correlation for our experimental data. At each temperature, ellipticity- and shift-derived rank orders correlate quite well, although three to four ellipticities deviate significantly. The correlation coefficients and standard deviations for linear regressions between sets of  $[\theta]_{222}$  and site 14 shifts lie within generally acceptable limits: 2 °C, 0.94, 1.4; 25 °C, 0.93, 1.0; 60 °C, 0.95, 0.4 (SD units are  $\text{deg cm}^2 \text{ dm}^{-1}$ ). These values show that this correlation is inferior to that seen for the closed squares of Figure 4; nonetheless, for many purposes, shifts and ellipticities provide nearly equivalent measures of helicity changes induced by a range of helix forming and breaking guests.

Since the above data correlations are not dependent on Lifson-Roig analyses, they might be said to maximize interpretational transparency, but they preclude one essential correlation, which is available if raw data are replaced by modeled propensities  $w_{\text{XXX}}/w_{\text{Ala}}$ , assigned using previously reported protocols.<sup>13,17,22c</sup> Figure 5 and Table 1 show the resulting correlations.

The correlation coefficients CC of column 5 are consistent with the previously cited, data-derived values of Figure 5, and columns 2 and 3 report intercepts and slopes of linear regressions carried out on paired  $w_{\text{XXX}}/w_{\text{Ala}}$  sets assigned at 2, 25, and 60 °C. Within assignment error, these are in quantitative agreement with the expected values of 0 and 1.0. These findings show that this pair of  $w_{\text{XXX}}/w_{\text{Ala}}$  sets passes normal correlation tests.<sup>36</sup> However, as seen in Figure 5, one additional important

correlation fails. For a majority of residues at 2 and 25 °C, the ellipticity-derived  $w_{\text{XXX}}/w_{\text{Ala}}$  are smaller than those calculated from shifts. This difference is expressed in the last Table 1 column as an averaged percentage of the shift-derived value. We attribute the consistently lower value of ellipticity-derived  $w_{\text{XXX}}/w_{\text{Ala}}$  assignments to guest-dependent decreases in the eq 3 calibration term  $[\theta]_{222,\text{H},n,T}$ . In so doing, we are reasoning from evidence that, unlike extinction coefficients of UV-vis spectroscopy, values of  $[\theta]_{222}$  are very sensitive to local structural perturbations. For example, the empirically assigned values for the parameter X of eq 2, used to assign length-dependence to  $[\theta]_{222,\text{H},n,T}$ , demonstrate this sensitivity. As shown in the Supporting Information, values for X allow calculation of the different contributions of an average end region alanine and a core alanine to the  $[\theta]_{222,\text{H},n,T}$  mean value. For the host, the end region value is 30–70% less than the core value.

A test of the validity of the two-state model that underlies Equation 1 is provided by temperature- and guest-dependent ellipticity values at 203 nm.<sup>37</sup> Superimposed plots of CD spectra for the host peptide at 2, 25, and 60 °C exhibit a well-defined isodichroic point at  $202.5 \pm 1 \text{ nm}$ , implying that as the temperature is increased from 2 to 60 °C, the constants  $[\theta]_{203,\text{H},n,T}$  and  $[\theta]_{203,\text{C},n,T}$  of eq 1 are equal and assume the expected literature intensity. If one adds to this plot the corresponding nine CD spectra of series **1** mutants containing the guests XXX = Nle, Nva, and Abu = α-aminobutyric acid, this isodichroic point remains invariant in both wavelength and intensity, as shown in the Supporting Information. However the temperature-dependent CD spectra of mutants containing guests with branched aliphatic side chains, rings, or polar side chains lack well-defined isodichroic points and exhibit intensity deviations at 203 nm of up to 30%. These ellipticities are inconsistent with a two-state helix-coil dichroic model.

In the Supporting Information, we further show that nearly all guest discrepancies of Figure 5 at 2 and 25 °C are consistent with decreases in  $[\theta]_{222,\text{H},n,T}$  that fall in the relatively narrow range of 5 to 15%. A larger decrease is seen for the Gly mutant. This is expected if glycine, with its unique conformational

(36) Myers, J. K.; Pace, C. N.; Scholtz, J. M. *Biochemistry* 1997, 36, 10923–10929.

(37) (a) Holtzer, M. H.; Holtzer, A. *Biopolymers* 1993, 32, 1675–1677. (b) Wallimann, P.; Kennedy, R. J.; Miller, J. S.; Shalongo, W.; Kemp, D. S. *J. Am. Chem. Soc.* 2002, 125, 1203–1220.

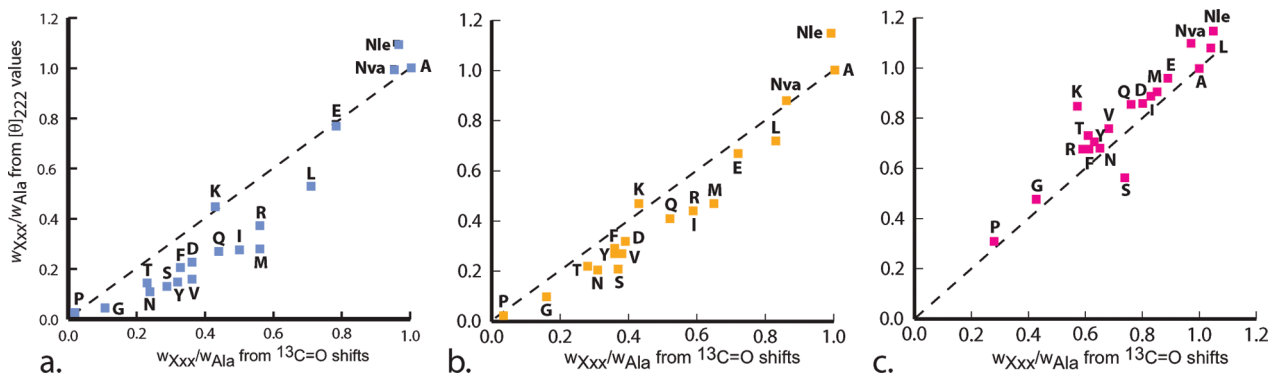


**Figure 5.** Squares define pairs of  $w_{Xxx}/w_{Ala}$ , assigned for each site 10 residue from  $[\theta]_{222}$  values, vertical axis and from  $^{13}\text{C}=\text{O}$  NMR chemical shifts, bottom axis. Temperatures: (a) 2 °C, (b) 25 °C, (c) 60 °C. Data were measured in  $\text{H}_2\text{O}$  (ellipticities) and in  $\text{D}_2\text{O}$  (shifts); for charged residues, shifts were measured in 10 mM Tris buffer,  $\text{pD} = 7.0$ . Shift-derived  $w_{Xxx}/w_{Ala}$  are averages of the assignments at sites 12, 14, and 15, and squares that lie on dashed lines correspond to  $w_{Xxx}/w_{Ala}$  values that are identical.

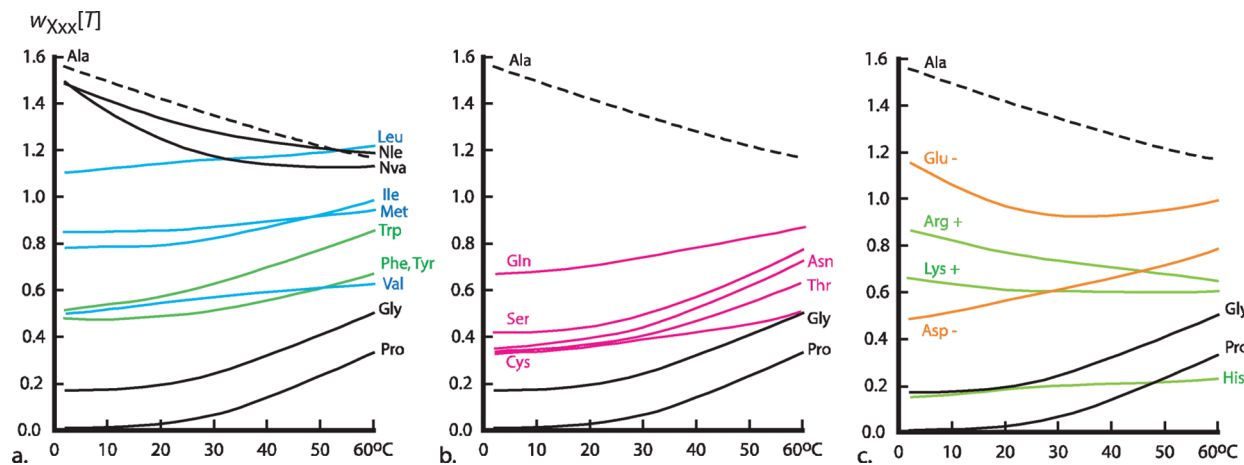


**Figure 6.** Interpolated  $w_{Xxx}[T]$  values assigned from the chemical shift-derived relative helical propensities  $w_{Xxx}/w_{Ala}$  of Figure 5 by  $w_{Ala}[T]$  multiplication followed by  $T$ -dependent quadratic fits as detailed in the Supporting Information. The depicted curves for  $w_{Ala}[T]$ ,  $w_{Nva}[T]$ ,  $w_{Gly}[T]$ , and  $w_{Pro}[T]$  have been reported previously.<sup>13</sup> See this report for a discussion of the problems that attend accurate assignment of  $w_{Pro}[T]$  at low temperatures.

freedom, induces an increase in local  $3_{10}$  helical character.<sup>38</sup> We conclude that for the natural amino acid residues, CD ellipticity data are valuable as confirmations of the  $^{13}\text{C}=\text{O}$  chemical shift-derived host–guest helical propensities, but by themselves, they lack the accuracy required for primary propensity assignments.

**Helical Propensities  $w_{Xxx}[T]$  for Amino Acids at a Central Site within a Polyalanine Context.<sup>39</sup>** Figure 6 depicts temperature-dependent helical propensities for twenty two amino acid residues, assigned in water within a polyalanine context. At 2 °C the propensity of alanine dominates. Its nearest competitor among the natural uncharged residues is leucine, but  $w_{Ala}[T]$  is 40% larger than  $w_{Leu}[T]$ , and in turn, this value is substantially larger than either  $w_{Met}[T]$  or  $w_{Ile}[T]$ . At 25 °C,  $w_{Ala}[T]$  is 30% larger than  $w_{Leu}[T]$ , but at 60 °C, within assignment error, these propensities are equal. Over the full temperature range, relatively large spacings between propensity values are characteristics of

the 2 °C assignments. With an increase in temperature, convergence occurs, reflecting in part the presence of both negative and positive slopes for key residues.

The alanine helical propensity decreases significantly and nearly linearly with temperature, and its values and slope are most closely matched by propensities for the two residues Nva and Nle that bear straight alkyl side chains.<sup>32</sup> Values for  $w_{Arg}[T]$  also decrease with a comparable slope, and perhaps coincidentally, the side chains of Arg and Nva share the same three-carbon backbone sequence. For the remaining fourteen uncharged residues, the slopes of the temperature dependences of their  $w_{Xxx}[T]$  values are positive. These are largest over the 25 to 60 °C interval, and expressed as percentages over the full range, the increases for the following residues are noteworthy: Trp: 67%, Ser: 83%, Thr: 85%, and Asn, 110%.

Large increases are also seen for the strong helix breakers Gly and Pro. At 2, 25, and 60 °C,  $w_{Ala}[T]/w_{Gly}[T]$  has respective values 9, 8, and 2.5, and the corresponding values for  $w_{Ala}[T]/w_{Pro}[T]$  are ≥100, 30, and 4. Since alanine is the strongest former and proline is the strongest breaker, these ratios define the full temperature-dependent propensity ranges, which decrease at least 25-fold as the temperature is raised from 2 to 60 °C.

What molecularly based conclusions can be drawn from these findings? Substantial prior effort has been directed toward

(38) (a) Long, H. F.; Tycko, R. *J. Am. Chem. Soc.* **1998**, *120*, 7039–7048. (b) Tomolo, C.; Polese, A.; Formaggio, F.; Crisma, M.; Kamphuis, J. *J. Am. Chem. Soc.* **1996**, *118*, 2744–2745.

(39) Other workers have reported helical propensities for guest residues within polyalanines or alanine-rich hosts. In addition to refs 12, 27b, and 27d, the following should be noted: (a) Zhou, N. E.; Monera, O. D.; Kay, C. M.; Hodges, R. S. *Protein Peptide Lett.* **1994**, *1*, 114–119. (b) Luo, P.; Baldwin, R. L. *Proc. Natl. Acad. Sci. U.S.A.* **1999**, *96*, 4930–4935.

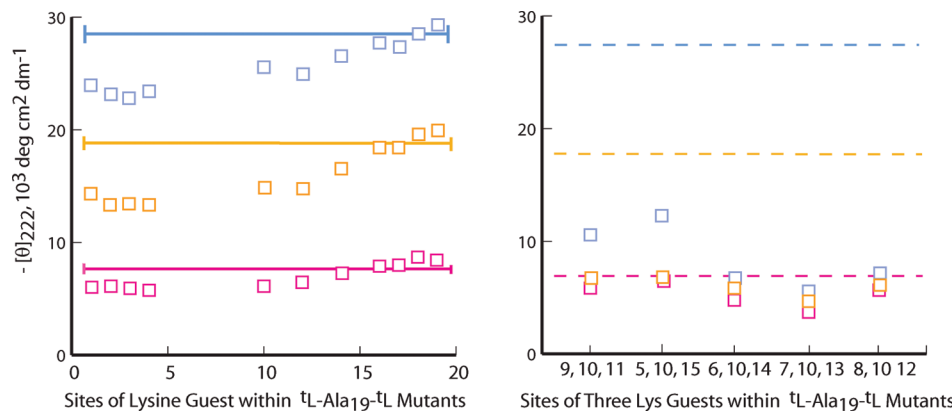


**Figure 7.** (a) Values of  $[\theta]_{222}$  for specifically sited single Lys<sup>+</sup> guests within the series **2** host at 2 °C (blue), 25 °C (orange), and 60 °C (magenta) at neutral pH in pure water. The solid lines correspond to values of  $[\theta]_{222}$  for the host. (b) Values of  $[\theta]_{222}$  for spaced pairs of Lys<sup>+</sup> guest triplets within this host at 2 °C (blue), 25 °C (orange), and 60 °C (magenta). The following helical propensities are assigned at 2 °C: for (a), single substitutions at sites 4, 10, and 16,  $w_{\text{Lys}}^2 = 0.54, 0.70, \geq 1.1$ . For the left-to-right triple substitutions of (b),  $\langle w_{\text{Lys}}^2 \rangle = 0.53, 0.56, 0.40, 0.37, 0.43$ . For these, the helicity rank order is thus:  $(i, i \pm 5) > (i, i \pm 1) > (i, i \pm 2) \geq (i, i \pm 4) > (i, i \pm 3)$ .

elucidation of aqueous helix–coil energetics,<sup>40</sup> and significant variables include residue-dependent coil entropies, coil and helix solvation energetics, and hydrophobic interactions<sup>41</sup> of the helical backbone with residue side chains. The residue- and temperature-dependent propensities of Figure 6 are at least qualitatively consistent with currently accepted thermodynamic models, yet none of the latter predict  $w_{\text{XXX}}[T]$  values quantitatively, and in a definitive recent overview Makhadze has suggested that computer simulation, rather than experiment, may provide an optimal future strategy.<sup>40</sup>

Helical propensities that take the form of rank-ordered lists of helix breakers and formers are widely used as heuristic tools for spotting helical and nonhelical regions within protein primary sequences. Three such lists, derived from the findings of this report, appear in the legend of Figure 4. We propose that these lists are likely to be most useful if they are supplemented by quantitative information that can be derived from Figure 5. Inspection of its three panels reveals clustered relative helical propensities (horizontal axes) for glutamine, aspartate, valine, tryptophan, phenylalanine, tyrosine, serine, asparagine, and threonine. At 2 °C, the mean propensity value for this cluster is  $0.33 \pm 0.07$ ; at 25 °C, the mean increases slightly to  $0.38 \pm 0.07$ ; but at 60 °C, the increase in this mean value is dramatic:  $0.68 \pm 0.08$ . Remarkably this effect is observed for both residues with nonpolar, hydrophobic side chains and for residues with short, polar side chains. Given appropriate local sequences, this mean magnitude is likely to be increased by stabilizing  $(i, i \pm 3)$  and  $(i, i \pm 4)$  context effects,<sup>20b</sup> suggesting that at high temperatures, a majority of residues may act as strong helix formers.

**Charged Residues.** Lysine data of Figure 7 provide a preliminary picture of helix-perturbing complexities caused by residues with charged side chains. It has long been recognized that host mutants derived from these residues are exceptions to the generalization that local effects dominate helical stability; for these residues, propensities are strongly site dependent.<sup>42</sup> Structurally speaking, a lysine residue is a norleucine in which a terminal  $\epsilon$ -hydrogen of the long, potentially flexible Nle chain

has been replaced by a charged  $-\text{NH}_3^+$  function. A comparison of ellipticities for the site scans of Figures 2a and 7a suggests that this terminal charge interacts with the helix backbone and on average, strongly diminishes the host helicity. In the earlier discussion of Figure 2a data, we noted the absence of detectable  $w_{\text{Nle}}[T]$  site dependences, and in Figure 2b we detected only hints of  $(i, i \pm 4)$  and  $(i, i \pm 3)$  context effects for mutants containing Nle pairs. The corresponding Figure 7a and b display dramatic site variations and evidence for local Lys-Lys energetic interactions that are helix-destabilizing. However, caution should be used in generalizing applications for these data, since they were measured in the absence of salt. At higher than physiological concentrations, sodium chloride has been shown to diminish the helix destabilizing interactions between alanine-rich sequences containing Lys- $\text{NH}_3^+$  functions.<sup>23</sup>

As detailed in the Supporting Information, these findings are shared by mutants containing the other residues that bear positively charged side chains. Allowing for the similar site-10 values for  $w_{\text{Lys}}[T]$  and  $w_{\text{Arg}}[T]$  and the much lower values seen in Figure 6 for  $w_{\text{His}}[T]$ , one finds that the site-dependent variations in ellipticities of Figure 2a are shared with corresponding Arg and His mutants. A dramatic increase in  $[\theta]_{222}$  intensity results if these guests are sited at any of the four C-terminal sequence residues, and this increase converges to a maximum at site 19. This is the expected signature of helix stabilization that results from placement of a positive charge near the C-terminal dipole of a helix backbone.<sup>43</sup>

Owing to these site and context dependences, helical propensities for central site charged residues provide at best a qualitative approximation to their range of helicity contributions at other sites. Histidine provides an extreme example. A recent PDB search of helical protein regions identified the 100 most frequently encountered four-residue sequences. All residues appear in these sequences, with the single exception of histidine.<sup>44</sup> Our data suggest an explanation. Over a full temperature range of our study, alone among charged residues, His consistently ranks among the four strongest helix breakers, unless it is sited at a C-terminus of a helical region.

A more general issue is posed by the large asymmetric influence of centrally sited charged residues on the relative

(40) Makhadze, G. I. *Adv. Protein Chem.* **2006**, 72, 199–226.

(41) Dill, K. A. *Biochemistry* **1990**, 29, 7133–7155.

(42) (a) Armstrong, K. M.; Baldwin, R. L. *Proc. Natl. Acad. Sci. U.S.A.* **1993**, 90, 11337–11340. (b) Hyghues-Despoines, G. M. P.; Scholtz, J. M.; Baldwin, R. L. *Protein Sci.* **1993**, 2, 1604–1611.

(43) Aqvist, J.; Lueke, H.; Quijano, F.; Warshel, A. *Proc. Natl. Acad. Sci. U.S.A.* **1991**, 88, 2026–2030.

(44) Acevedo, O. E.; Lareo, L. R. *OMICS* **2005**, 9, 391–399.

weighting of ensemble conformations. Specifically, at 2 °C, the central site  $w_{\text{Lys}}[2]$  values lie above 1.6 for all conformations with helical regions that terminate at that site, but its values for conformations that are initiated or continued at that site are smaller by about a factor of 3. As a result, for sequences of medium length in which charge-derived context effects are minor, a central substitution by a charged Lys, Arg, or His residue will substantially skew site helicities to favor the N-terminal half of the sequence. Owing to averaging, an FH is relatively insensitive to this effect, but  $\text{FH}_i$  values, assigned at a pair of sites that are spaced equally from a central charged residue, will be skewed to lower or to higher relative values, depending upon the charge sign, and judiciously sited  $^{13}\text{C}=\text{O}$ -labeled alanines should allow experimental characterization of this helicity-biasing effect.

**Comparison of Two Temperature-Dependent Helical Propensity Sets; Summary.** As noted above, the Scheraga group previously reported helical propensities for a large temperature range using mutants of oligopeptide hosts that were constructed from  $\text{N}^5-(3-hydroxypropyl)- and  $\text{N}^5$ -(4-hydroxybutyl)-L-glutamine residues. The linear side chains of the resulting hosts contain five or six methylenes, polar secondary amides and polar hydroxyl functions at their termini. Conformational side chain diversity is thus a likely host feature. In addition to flexibility attributable to the normal gauche-anti conformers of alkyl regions, conformational freedom at the single amide-linked  $\text{C}-\text{C}=\text{O}$  and  $\text{C}-\text{NH}$  bonds that appear near the side chain centers should resemble the permissive glycine  $\Psi$  and  $\phi$  values. Some of the coil state freedom is lost in a coil–helix transition, but side chain motion is likely to be retained in helical conformations. Hydrophobic and/or polar context effects are thus expected for guests introduced within these hosts,<sup>45</sup> and conceivably, retained conformational diversity in the helical state may increase with temperature, with a resulting increase in the crowding of bulky guest side chains.$

A new test of fit is appropriate if, as seen in the 2 °C plot of Figure 6, propensities for alanine, glycine, and proline are distanced from those of their neighbors. This test excludes the outliers and compares the means of values for the remaining propensities. For the Figure 6 assignments these means are: 2 °C 0.65; 25 °C 0.65; 60 °C 0.84, and the analogous means for the Scheraga propensities are: 2 °C 0.98; 25 °C 0.95; 60 °C 0.86. At 2 and 25 °C, the latter exceed the former by 50%, suggesting the presence of helix stabilizing context effects within the Scheraga hosts. Also informative are comparisons for pairs of residue values. Inspection of Figure 6 shows that as the temperature is increased from 2 to 60 °C,  $w_{\text{XXX}}[T]$  for alanine, arginine<sup>+</sup>, and glutamate decrease by 15–25%; the values for histidine remain constant, and values increase significantly for the set that includes the remaining natural residues. For glycine, proline, asparagine, threonine, valine, and serine at 0–40 °C, the Scheraga propensities also increase with temperature. For alanine, leucine, phenylalanine, cysteine, and lysine<sup>+</sup>, the Scheraga propensities decrease slightly or are constant with a small maximum, but for the remaining nine residues these propensities decrease by 15–55%. Relatively speaking, for these guests, the Scheraga hosts become less hospitable as the temperature is raised.

Figure 8 correlates the 60 °C Scheraga propensities with those assigned in the minimally interactive polyalanine host. A poor

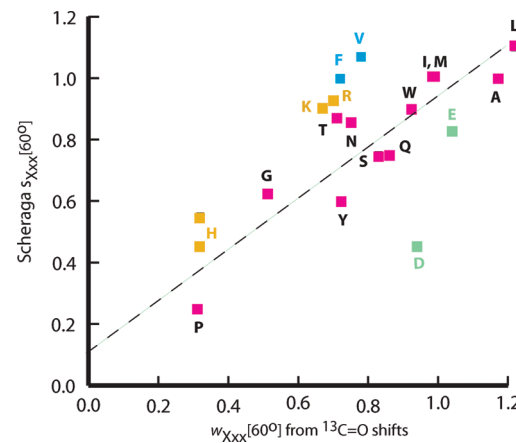


**Figure 8.** Comparison of 60 °C helical propensity sets. The vertical axis plots Scheraga  $s$  values<sup>9c</sup> versus Figure 6  $w_{\text{XXX}}[T]$  values, horizontal axis. Vertical His and His<sup>+</sup> values are both depicted; the Figure 6 His value was assigned at pH 7. The correlation coefficient for all residues is 0.68; it increases to 0.91 if data for F, V, and the charged residues are excluded.

correlation is seen for the five residues with charged side chains and is likely attributable to the high context sensitivity of members of this residue class. For valine and phenylalanine the Scheraga propensities lie substantially above the correlation line, but not outside of the plausible range of hydrophobic context effects reported by Creamer and Rose.<sup>20b</sup> If propensities for these seven residues are excluded, the comparison passes correlation coefficient and slope tests. The overall quality of correlation at 60 °C thus reveals the dominant operation of helical propensity differences, even in the presence of potentially large context effects.

At 2 and 25 °C, the interpretive significance of slopes and correlation coefficients are compromised by the outlier properties of  $w_{\text{Ala}}[T]$ ,  $w_{\text{Gly}}[T]$ , and  $w_{\text{Pro}}[T]$ .<sup>46</sup> Examination of the temperature-dependent values of the ratios  $w_{\text{Ala}}[T]/w_{\text{Gly}}[T]$  and  $w_{\text{Ala}}[T]/w_{\text{Pro}}[T]$  reveals the problem. At 2 °C, our  $w_{\text{Ala}}[T]/w_{\text{Pro}}[T]$  ratio is at least 100, but the Scheraga ratio is ca. 15; at 25 °C the corresponding ratios are 30 and 5; but at 60 °C, they converge to 4 and 3. At 2 °C, our  $w_{\text{Ala}}[T]/w_{\text{Gly}}[T]$  ratio is 9, but the Scheraga ratio is ca. 2.1; at 25 °C the corresponding ratios are 8 and 1.8; but at 60 °C, they converge to 2.4 and 1.6.

Context corrections that arise in typical helical sequences derived from globular proteins are likely to reduce our high outlier  $w_{\text{Ala}}[T]$  and our low outlier  $w_{\text{Gly}}[T]$  values. In a recent report,<sup>13</sup> we used spaced, solubilized, spaced mutants <sup>1</sup>Leu<sub>3</sub>-AlaNva<sub>4</sub>XxxNva<sub>4</sub>Ala<sub>9</sub><sup>+</sup>Leu<sub>3</sub> to reassign these propensities within a local polynorvaline context, which embodies host–guest hydrophobic  $\beta$ -,  $\gamma$ -, and  $\delta$ -CH contacts. The resulting context-dependent  $w_{\text{Gly}}[T]$  converge to 0.5 at all temperatures, and in the range 25–60 °C,  $w_{\text{Ala}}[T]$  decreases from ca. 1.2 to 1.0. These are close to the Scheraga values.

We have here reported the first context-independent, temperature-dependent helical propensity sets for the natural and for selected other amino acid residues. These sets and the methodology used in their assignments jointly provide a rigorous foundation for further studies. Our most important result is the

(46) The slope and CC linearity tests are maximally sensitive to deviations in randomly selected data points only if the data sets are nearly evenly spaced. A good approximation to this ideal is seen in Figure 8. If one or both sets must be characterized as a central data cluster with high and low outliers, values for CC and slope yield only a three-point correlation: high value, mean value for cluster, low value.

(45) See reference 20a for data derived from peptide host experiments that provide insight into this issue.

demonstration that in a polyalanine context, the helix-forming tendencies of the large majority of natural amino acid residues increase significantly as the temperature is raised. This result implies a substantial increase in the percentage of natural residues that can act as helix formers.

As we have noted in the introduction, characterization at a chemical level of the dependencies of peptide helicity on residue composition and sequence requires assignment of temperature-dependences for both propensities and a linked set of context dependences. For the latter assignments, the series **1** polyalanine mutants are ideally suited, owing to a substantial length region that can accommodate pairs of guests. The practical consequences of our Figure 6 findings include a more satisfactory foundation for molecular modeling experiments, a better predictive understanding of the effects of site mutations on early folding intermediates that have been linked to human degenerative diseases, and practical insights into protein stability for living organisms that include mesophiles and thermophiles. Although 80 °C almost certainly defines the practical upper limit for guest mutation studies in hosts of structure **1**, the  $w_{\text{Ala}}[T]$  value near 1.1 that we have assigned at 80 °C suggests the feasibility of using hosts with considerably longer lengths. In effect, one should be able to apply lessons from the extensive prior oligopeptide methodology to spaced, solubilized polyalanines. Moreover, the practical aqueous temperature limit of 100 °C may be extendable through use of additives such as ethylene glycol, which we have previously utilized to carry out low temperature CD studies.<sup>15</sup>

## Experimental Section

**Synthesis, Purification, and Characterization of Peptides.** Peptides **1** and **2** were synthesized on a 0.02–0.03 mmol scale using a PE Biosystems Pioneer Peptide Synthesizer with standard 9-fluorenylmethyleneoxy-carbonyl (Fmoc/HBTU) chemistry.<sup>14f</sup> and peptides were cleaved from the resin as reported previously.<sup>14f,h,15</sup> For unlabeled couplings, 9 equiv of Fmoc–AA–OH and HATU were used. For <sup>13</sup>C=O labeled sites, HBTU and three equivalents of a mixture of labeled and nonlabeled Fmoc–Ala–OH with <sup>13</sup>C percentages that varied from 100% to 25% were used and each labeled site was then double-coupled with 9 equiv of nonlabeled Fmoc–Ala–OH. Purification was carried out on a Waters 2690 HPLC with autoinjector and 996 detector using YMC ODS-AQ 200 Å 4.5 × 150 mm columns. Further details concerning preparation and characterization of peptides **2** appear in ref 14h.

**NMR Experiments.** Peptide **1** samples containing uncharged guest residues were analyzed unbuffered in pure D<sub>2</sub>O at concentra-

tions of 1 to 2 mM; for peptides containing charged guests, 10 mM Tris buffer (pD = 7.0) was used. The <sup>13</sup>C spectra were collected using VNMR 6.1c software on a Varian Inova-500 MHz NMR spectrometer, equipped with an Oxford Instruments superconducting magnet and a 5 mm dual broadband RF (50–202 MHz), CP/MS <sup>13</sup>C–<sup>31</sup>P{<sup>1</sup>H} solids probe. Proton-decoupled carbon resonance spectra were measured at temperatures of 2, 25, and 60 °C. Probe temperatures were maintained by a Varian variable temperature unit and calibrated using 100% methanol for the range 1–40 °C and ethylene glycol at 60 °C according to instructions provided by Varian. The calibrated values agree within 1 °C with values reported by Van Geet.<sup>47</sup> For all experiments, the <sup>13</sup>C chemical shifts were referenced at each temperature relative to 0.1 M DSS (sodium 2,2-dimethyl-2-silapentane-5-sulfonate) by setting its <sup>1</sup>H methyl shift value to zero.<sup>48</sup> The assigned <sup>13</sup>C=O chemical shift values of this report appear in the Supporting Information.

**Circular Dichroism Experiments.** UV spectra of solutions of peptides **2** in 18.2 MΩ water were measured on a double-beam Varian Cary 100 Bio UV–visible spectrophotometer, and their concentrations were assigned using the Trp UV chromophore with molar absorptivity at 280 nm of 5560 cm<sup>-1</sup> M<sup>-1</sup>.<sup>14h</sup> All peptides exhibited a normal peak shape for the Trp chromophore. CD spectra were measured at ca. 12 mM peptide concentrations using a single-beam Aviv 62DS spectropolarimeter equipped with a thermostatic temperature controller that was calibrated using d-10-camphorsulfonic acid. Peptides containing charged guests were studied in pH 1.2 and pH 7 phosphate buffers. CD spectra were measured after twelve-minute temperature equilibrations in 10 mm Hellma QS strain-free suprasil cells. Five successive spectra, 195–255 nm, were measured at 1.0 nm bandwidth and 0.5 nm step size, averaged, and smoothed using Aviv 62DS version 4.0 software. The Supporting Information contains peptide [θ]<sub>222</sub> values cited in the text.

**Acknowledgment.** We thank the NIH, Grant GM 13453, for generous support.

**Supporting Information Available:** Peptides **1** and **2** mass spectroscopic molecular ions; peptide **1** <sup>13</sup>C=O chemical shifts; peptide **2** ellipticities [θ]<sub>222</sub>; helical propensity assignments; detailed analysis of systematic errors in helicities calculated from [θ]<sub>222</sub> data. This material is available free of charge via the Internet at <http://pubs.acs.org>.

JA904271K

(47) Van Geet, A. L. *Anal. Chem.* **1968**, *40*, 2227–2229.

(48) Markley, J. L.; Bax, A.; Arata, Y.; Hilbers, C. W.; Kaptein, R.; Sykes, B. D.; Wright, P. E.; Wüthrich, K. *Pure Appl. Chem.* **1998**, *70*, 117–142.

**Supporting Information for Moreau, Schubert, Nasr, Török, Miller, Kennedy, Kemp:**

“Context-Independent, Temperature-Dependent Helical Propensities for Amino Acid Residues.”

**I. Circular Dichroism Data**

A. Norleucine scan

peptide 2	-[θ] <sub>222</sub> deg cm <sup>2</sup> dmol <sup>-1</sup>	2°C	25°C	60°C
WK <sub>4</sub> Inp <sub>2</sub> 'LNleA <sub>18</sub> 'LInp <sub>2</sub> K <sub>4</sub> NH <sub>2</sub>	27844	18765	7750	
WK <sub>4</sub> Inp <sub>2</sub> 'LANleA <sub>17</sub> 'LInp <sub>2</sub> K <sub>4</sub> NH <sub>2</sub>	28975	18341	7394	
WK <sub>4</sub> Inp <sub>2</sub> 'LA <sub>2</sub> NleA <sub>16</sub> 'LInp <sub>2</sub> K <sub>4</sub> NH <sub>2</sub>	27579	18217	7233	
WK <sub>4</sub> Inp <sub>2</sub> 'LA <sub>3</sub> NleA <sub>15</sub> 'LInp <sub>2</sub> K <sub>4</sub> NH <sub>2</sub>	30339	20298	8120	
WK <sub>4</sub> Inp <sub>2</sub> 'LA <sub>5</sub> NleA <sub>13</sub> 'LInp <sub>2</sub> K <sub>4</sub> NH <sub>2</sub>	27816	19068	7813	
WK <sub>4</sub> Inp <sub>2</sub> 'LA <sub>7</sub> NleA <sub>11</sub> 'LInp <sub>2</sub> K <sub>4</sub> NH <sub>2</sub>	28620	18815	7444	
WK <sub>4</sub> Inp <sub>2</sub> 'LA <sub>9</sub> NleA <sub>9</sub> 'LInp <sub>2</sub> K <sub>4</sub> NH <sub>2</sub>	28872	18798	7728	
WK <sub>4</sub> Inp <sub>2</sub> 'LA <sub>11</sub> NleA <sub>7</sub> 'LInp <sub>2</sub> K <sub>4</sub> NH <sub>2</sub>	28243	18134	7322	
WK <sub>4</sub> Inp <sub>2</sub> 'LA <sub>13</sub> NleA <sub>5</sub> 'LInp <sub>2</sub> K <sub>4</sub> NH <sub>2</sub>	28316	18422	7357	
WK <sub>4</sub> Inp <sub>2</sub> 'LA <sub>15</sub> NleA <sub>3</sub> 'LInp <sub>2</sub> K <sub>4</sub> NH <sub>2</sub>	28851	18590	7627	
WK <sub>4</sub> Inp <sub>2</sub> 'LA <sub>16</sub> NleA <sub>2</sub> 'LInp <sub>2</sub> K <sub>4</sub> NH <sub>2</sub>	27745	17947	7405	
WK <sub>4</sub> Inp <sub>2</sub> 'LA <sub>17</sub> NleA'LInp <sub>2</sub> K <sub>4</sub> NH <sub>2</sub>	27900	18124	7598	
WK <sub>4</sub> Inp <sub>2</sub> 'LA <sub>18</sub> Nle'LInp <sub>2</sub> K <sub>4</sub> NH <sub>2</sub>	29162	19212	7728	

B. Double Norleucine scan

	2°C	25°C	60°C
WK <sub>4</sub> Inp <sub>2</sub> <sup>t</sup> LA <sub>9</sub> Nle <sub>2</sub> A <sub>8</sub> <sup>t</sup> LInp <sub>2</sub> K <sub>4</sub> NH <sub>2</sub>	28066	17309	7466
WK <sub>4</sub> Inp <sub>2</sub> <sup>t</sup> LA <sub>8</sub> NleANleA <sub>8</sub> <sup>t</sup> LInp <sub>2</sub> K <sub>4</sub> NH <sub>2</sub>	27573	17264	7204
WK <sub>4</sub> Inp <sub>2</sub> <sup>t</sup> LA <sub>8</sub> NleA <sub>2</sub> NleA <sub>7</sub> <sup>t</sup> LInp <sub>2</sub> K <sub>4</sub> NH <sub>2</sub>	26489	16843	7342
WK <sub>4</sub> Inp <sub>2</sub> <sup>t</sup> LA <sub>7</sub> NleA <sub>3</sub> NleA <sub>7</sub> <sup>t</sup> LInp <sub>2</sub> K <sub>4</sub> NH <sub>2</sub>	29313	19404	8408
WK <sub>4</sub> Inp <sub>2</sub> <sup>t</sup> LA <sub>6</sub> NleA <sub>4</sub> NleA <sub>7</sub> <sup>t</sup> LInp <sub>2</sub> K <sub>4</sub> NH <sub>2</sub>	28321	17664	7353
WK <sub>4</sub> Inp <sub>2</sub> <sup>t</sup> LA <sub>5</sub> NleA <sub>7</sub> NleA <sub>5</sub> <sup>t</sup> LInp <sub>2</sub> K <sub>4</sub> NH <sub>2</sub>	28223	18262	7671
WK <sub>4</sub> Inp <sub>2</sub> <sup>t</sup> LA <sub>2</sub> NleA <sub>13</sub> NleA <sub>2</sub> <sup>t</sup> LInp <sub>2</sub> K <sub>4</sub> NH <sub>2</sub>	27398	18080	7725

C. Double Norvaline scan

	2°C	25°C	60°C
WK <sub>4</sub> Inp <sub>2</sub> <sup>t</sup> LA <sub>9</sub> Nva <sub>2</sub> A <sub>8</sub> <sup>t</sup> LInp <sub>2</sub> K <sub>4</sub> NH <sub>2</sub>	26089	15519	6596
WK <sub>4</sub> Inp <sub>2</sub> <sup>t</sup> LA <sub>8</sub> NvaANvaA <sub>8</sub> <sup>t</sup> LInp <sub>2</sub> K <sub>4</sub> NH <sub>2</sub>	26211	15650	6610
WK <sub>4</sub> Inp <sub>2</sub> <sup>t</sup> LA <sub>8</sub> NvaA <sub>2</sub> NvaA <sub>7</sub> <sup>t</sup> LInp <sub>2</sub> K <sub>4</sub> NH <sub>2</sub>	24274	14660	6161
WK <sub>4</sub> Inp <sub>2</sub> <sup>t</sup> LA <sub>7</sub> NvaA <sub>3</sub> NvaA <sub>7</sub> <sup>t</sup> LInp <sub>2</sub> K <sub>4</sub> NH <sub>2</sub>	27222	17311	7330
WK <sub>4</sub> Inp <sub>2</sub> <sup>t</sup> LA <sub>6</sub> NvaA <sub>4</sub> NvaA <sub>7</sub> <sup>t</sup> LInp <sub>2</sub> K <sub>4</sub> NH <sub>2</sub>	26698	16166	6999
WK <sub>4</sub> Inp <sub>2</sub> <sup>t</sup> LA <sub>5</sub> NvaA <sub>7</sub> NvaA <sub>5</sub> <sup>t</sup> LInp <sub>2</sub> K <sub>4</sub> NH <sub>2</sub>	27092	16638	7023
WK <sub>4</sub> Inp <sub>2</sub> <sup>t</sup> LA <sub>2</sub> NvaA <sub>13</sub> NvaA <sub>2</sub> <sup>t</sup> LInp <sub>2</sub> K <sub>4</sub> NH <sub>2</sub>	26442	16915	7171

D. Single and double Guests WK<sub>4</sub>Inp<sub>2</sub><sup>t</sup>LNleA<sub>9</sub>XA<sub>9</sub><sup>t</sup>Li<sub>n</sub>p<sub>2</sub>K<sub>4</sub>NH<sub>2</sub> WK<sub>4</sub>Inp<sub>2</sub><sup>t</sup>LNleA<sub>9</sub>X<sub>2</sub>A<sub>8</sub><sup>t</sup>Li<sub>n</sub>p<sub>2</sub>K<sub>4</sub>NH<sub>2</sub>  
 -[θ]<sub>222</sub> deg cm<sup>2</sup> dmol<sup>-1</sup> Guest X

Guest	2°C	25°C	60°C	double Guest	2°C	25°C	60°C
Pro	1346	2406	3236				
Gly	12828	7127	4285	GG	3925	3568	3429
Val	21366	12056	5719	VV	13509	7157	4419
Phe	22617	12688	5288	FF	13438	7372	4048
Ser-OMe	23835	13322	5385	(S-OMe) <sub>2</sub>	17349	8590	4203
Ile	24035	14578	6303	II	19289	10906	5681
Met	24048	14855	6374	MM	20615	12601	5888
Abu	26323	16123	6485	Abu <sub>2</sub>	23103	13006	5486
Leu	26162	16701	7073	7357	24143	15092	6813
Ala	27464	17757	6825	7627	27464	15519	6825
Nva	27791	17353	7247	Nva <sub>2</sub>	27464	17757	6596
Nle	28872	18798	7728	Nle <sub>2</sub>	28066	17697	7466
Asn	18993	10685	5302	NN	10252	6488	4622
Ser	19920	10912	4726	SS	11317	6517	4710
Thr	20549	11057	5551	TT	9513	4551	4386
Tyr	20930	12220	5533	YY	11922	6979	3715
Gln	23943	14152	6232	QQ	17266	10021	4760

E. Lysine pH 7, Arginine pH 7, Histidine pH 1.2

peptide 2	$-\text{[}\theta\text{]}_{222} \text{ deg cm}^2 \text{ dmol}^{-1}$	2°C	25°C	60°C
WK <sub>4</sub> Inp <sub>2</sub> 'LLysA <sub>18</sub> 'LInp <sub>2</sub> K <sub>4</sub> NH <sub>2</sub>	24035	14436	6123	
WK <sub>4</sub> Inp <sub>2</sub> 'LALysA <sub>17</sub> 'LInp <sub>2</sub> K <sub>4</sub> NH <sub>2</sub>	23168	13484	6189	
WK <sub>4</sub> Inp <sub>2</sub> 'LA <sub>2</sub> LysA <sub>16</sub> 'LInp <sub>2</sub> K <sub>4</sub> NH <sub>2</sub>	22857	13453	5889	
WK <sub>4</sub> Inp <sub>2</sub> 'LA <sub>3</sub> LysA <sub>15</sub> 'LInp <sub>2</sub> K <sub>4</sub> NH <sub>2</sub>	23532	13375	5754	
WK <sub>4</sub> Inp <sub>2</sub> 'LA <sub>9</sub> LysA <sub>9</sub> 'LInp <sub>2</sub> K <sub>4</sub> NH <sub>2</sub>	25582	14866	6154	
WK <sub>4</sub> Inp <sub>2</sub> 'LA <sub>11</sub> LysA <sub>7</sub> 'LInp <sub>2</sub> K <sub>4</sub> NH <sub>2</sub>	24997	14817	6566	
WK <sub>4</sub> Inp <sub>2</sub> 'LA <sub>13</sub> LysA <sub>5</sub> 'LInp <sub>2</sub> K <sub>4</sub> NH <sub>2</sub>	26565	16622	7198	
WK <sub>4</sub> Inp <sub>2</sub> 'LA <sub>15</sub> LysA <sub>3</sub> 'LInp <sub>2</sub> K <sub>4</sub> NH <sub>2</sub>	27835	18293	8021	
WK <sub>4</sub> Inp <sub>2</sub> 'LA <sub>16</sub> LysA <sub>2</sub> 'LInp <sub>2</sub> K <sub>4</sub> NH <sub>2</sub>	27371	18382	8043	
WK <sub>4</sub> Inp <sub>2</sub> 'LA <sub>17</sub> NleA'LInp <sub>2</sub> K <sub>4</sub> NH <sub>2</sub>	28597	19703	8678	
WK <sub>4</sub> Inp <sub>2</sub> 'LA <sub>18</sub> Lys'LInp <sub>2</sub> K <sub>4</sub> NH <sub>2</sub>	29284	20029	8328	
WK <sub>4</sub> Inp <sub>2</sub> 'LArgA <sub>18</sub> 'LInp <sub>2</sub> K <sub>4</sub> NH <sub>2</sub>	22419	13118	4994	
WK <sub>4</sub> Inp <sub>2</sub> 'LA <sub>4</sub> ArgA <sub>14</sub> 'LInp <sub>2</sub> K <sub>4</sub> NH <sub>2</sub>	22006	12016	4421	
WK <sub>4</sub> Inp <sub>2</sub> 'LA <sub>9</sub> ArgA <sub>9</sub> 'LInp <sub>2</sub> K <sub>4</sub> NH <sub>2</sub>	24321	14644	5296	
WK <sub>4</sub> Inp <sub>2</sub> 'LA <sub>12</sub> ArgA <sub>6</sub> 'LInp <sub>2</sub> K <sub>4</sub> NH <sub>2</sub>	26244	16623	6571	
WK <sub>4</sub> Inp <sub>2</sub> 'LA <sub>15</sub> ArgA <sub>3</sub> 'LInp <sub>2</sub> K <sub>4</sub> NH <sub>2</sub>	27013	18068	7266	
WK <sub>4</sub> Inp <sub>2</sub> 'LA <sub>18</sub> Arg'LInp <sub>2</sub> K <sub>4</sub> NH <sub>2</sub>	28142	19271	7604	
WK <sub>4</sub> Inp <sub>2</sub> 'LA <sub>4</sub> HisA <sub>14</sub> 'LInp <sub>2</sub> K <sub>4</sub> NH <sub>2</sub>	17611	9046	3177	
WK <sub>4</sub> Inp <sub>2</sub> 'LA <sub>9</sub> HisA <sub>9</sub> 'LInp <sub>2</sub> K <sub>4</sub> NH <sub>2</sub>	17620	9259	3374	
WK <sub>4</sub> Inp <sub>2</sub> 'LA <sub>12</sub> HisA <sub>6</sub> 'LInp <sub>2</sub> K <sub>4</sub> NH <sub>2</sub>	26244	16623	6008	
WK <sub>4</sub> Inp <sub>2</sub> 'LA <sub>15</sub> HisA <sub>3</sub> 'LInp <sub>2</sub> K <sub>4</sub> NH <sub>2</sub>	27013	18068	7266	
WK <sub>4</sub> Inp <sub>2</sub> 'LA <sub>18</sub> His'LInp <sub>2</sub> K <sub>4</sub> NH <sub>2</sub>	27733	18800	8642	
WK <sub>4</sub> Inp <sub>2</sub> 'LA <sub>9</sub> GluA <sub>9</sub> 'LInp <sub>2</sub> K <sub>4</sub> NH <sub>2</sub>	26364	14162	6232 pH 1.2	
WK <sub>4</sub> Inp <sub>2</sub> 'LA <sub>9</sub> GluA <sub>9</sub> 'LInp <sub>2</sub> K <sub>4</sub> NH <sub>2</sub>	26539	16360	6609 pH 7	
WK <sub>4</sub> Inp <sub>2</sub> 'LA <sub>9</sub> AspA <sub>9</sub> 'LInp <sub>2</sub> K <sub>4</sub> NH <sub>2</sub>	20929	11438	4694 pH 1.2	
WK <sub>4</sub> Inp <sub>2</sub> 'LA <sub>9</sub> AspA <sub>9</sub> 'LInp <sub>2</sub> K <sub>4</sub> NH <sub>2</sub>	23174	12986	6198 pH 7	

F. Double and Triple Lysine scan

	2°C	25°C	60°C
WK <sub>4</sub> Inp <sub>2</sub> <sup>t</sup> LA <sub>8</sub> K <sub>3</sub> A <sub>8</sub> <sup>t</sup> LInp <sub>2</sub> K <sub>4</sub> NH <sub>2</sub>	10510	6154	6072
WK <sub>4</sub> Inp <sub>2</sub> <sup>t</sup> LA <sub>7</sub> KAKAKA <sub>7</sub> <sup>t</sup> LInp <sub>2</sub> K <sub>4</sub> NH <sub>2</sub>	7263	4673	5463
WK <sub>4</sub> Inp <sub>2</sub> <sup>t</sup> LA <sub>6</sub> KA <sub>2</sub> KA <sub>2</sub> KA <sub>6</sub> <sup>t</sup> LInp <sub>2</sub> K <sub>4</sub> NH <sub>2</sub>	5638	4039	5100
WK <sub>4</sub> Inp <sub>2</sub> <sup>t</sup> LA <sub>5</sub> KA <sub>3</sub> KA <sub>3</sub> KA <sub>5</sub> <sup>t</sup> LInp <sub>2</sub> K <sub>4</sub> NH <sub>2</sub>	6874	4583	5920
WK <sub>4</sub> Inp <sub>2</sub> <sup>t</sup> LA <sub>4</sub> KA <sub>4</sub> KA <sub>4</sub> KA <sub>4</sub> <sup>t</sup> LInp <sub>2</sub> K <sub>4</sub> NH <sub>2</sub>	12273	7030	6561
WK <sub>4</sub> Inp <sub>2</sub> <sup>t</sup> LA <sub>6</sub> KA <sub>5</sub> KA <sub>6</sub> <sup>t</sup> LInp <sub>2</sub> K <sub>4</sub> NH <sub>2</sub>	18159	10835	7799
WK <sub>4</sub> Inp <sub>2</sub> <sup>t</sup> LA <sub>8</sub> KAKA <sub>8</sub> <sup>t</sup> LInp <sub>2</sub> K <sub>4</sub> NH <sub>2</sub>	18018	10015	6897

## **II. Molecular Ion MS Data for Series 2 Peptides**

<u>Peptide</u>	<u>m/z Found (Expected)</u>
NleA14	753.26 (752.48), 602.80 (602.19), 502.52 (501.99), 430.90 (430.42), 377.17 (376.75)
ANleA13	753.23 (752.48), 602.78 (602.19), 502.52 (501.99), 430.88 (430.42), 377.06 (376.75)
A2NleA12	1003.98 (1002.98), 753.38 (752.48), 602.80 (602.19), 502.52 (501.99), 430.90 (430.42), 377.17 (376.75)
A3NleA11	1003.98 (1002.98), 753.26 (752.48), 602.80 (602.19), 502.52 (501.99), 430.90 (430.42), 377.17 (376.75)
A5NleA9	753.16 (752.48), 602.72 (602.19), 502.52 (501.99), 430.81 (430.42), 377.00 (376.75)
A7NleA7	1003.79 (1002.98), 753.38 (752.48), 602.87 (602.19), 502.52 (501.99), 430.96 (430.42), 377.17 (376.75)
A9NleA5	753.45 (752.48), 602.93 (602.19), 502.71 (501.99), 430.96 (430.42), 377.17 (376.75)
A11NleA3	753.23 (752.48), 602.85 (602.19), 502.52 (501.99), 430.88 (430.42), 377.19 (376.75), 251.66 (251.50)
A12NleA2	602.52 (602.19), 502.26 (501.99), 430.68 (430.42), 376.86 (376.75), 251.46 (251.50)
A13NleA	1003.85 (1002.98), 753.52 (752.48), 602.80 (602.19), 502.52 (501.99), 430.90 (430.42), 377.17 (376.75)
A14Nle	1004.17 (1002.98), 753.20 (752.48), 602.80 (602.19), 502.58 (501.99), 430.90 (430.42), 377.11 (376.75)
NleA18	659.55 (659.02), 549.82 (549.35), 471.34 (471.02), 412.52 (412.26)
ANleA17	659.62 (659.02), 549.82 (549.35), 471.34 (471.02), 412.65 (412.26)
A2NleA16	659.55 (659.02), 550.02 (549.35), 471.47 (471.02), 412.72 (412.26)
A3NleA15	824.43 (823.52), 659.77 (659.02), 549.95 (549.35), 471.54 (471.02), 412.76 (412.26)
A5NleA13	549.95 (549.35), 471.54 (471.02), 412.72 (412.26)
A7NleA11	659.69 (659.02), 549.95 (549.35), 471.54 (471.02), 412.65 (412.26)
A2NleA13NleA2	667.81 (667.43), 556.43 (556.36), 477.09 (477.02), 417.56 (417.52)
A5NleA7NleA5	668.07 (667.43), 556.81 (556.36), 477.53 (477.02), 417.94 (417.52)
A6NleA4NleA6	668.01 (667.43), 556.81 (556.36), 477.47 (477.02), 417.88 (417.52)

A7NleA3NleA7	667.94 (667.43), 556.75 (556.36), 477.35 (477.02), 417.82 (417.52)
A8NleA2NleA7	668.07 (667.43), 556.81 (556.36), 477.53 (477.02), 417.94 (417.52)
A8NleANleA8	667.62 (667.43), 556.43 (556.36), 477.09 (477.02), 417.56 (417.52)
A9NleNleA8	668.07 (667.43), 556.94 (556.36), 477.47 (477.02), 418.01 (417.52)
A2NvaA13NvaA2	662.08 (661.82), 551.88 (551.69), 473.22 (473.02), 414.20 (414.02)
A5NvaA7NvaA5	827.42 (827.03), 662.08 (661.82), 551.88 (551.69), 473.22 (473.02), 414.20 (414.02)
A6NvaA4NvaA6	827.55 (827.03), 662.26 (661.82), 551.94 (551.69), 473.35 (473.02), 414.26 (414.02)
A7NvaA3NvaA7	827.55 (827.03), 662.14 (661.82), 551.94 (551.69), 473.22 (473.02), 414.20 (414.02)
A8NvaA2NvaA7	827.98 (827.03), 662.58 (661.82), 552.32 (551.69), 473.60 (473.02), 414.51 (414.02)
A8NvaANvaA8	827.36 (827.03), 662.14 (661.82), 551.94 (551.69), 473.16 (473.02), 414.20 (414.02)
A9NvaNvaA8	827.74 (827.03), 662.45 (661.82), 552.19 (551.69), 473.41 (473.02), 414.38 (414.02)
A9NvaA9	820.76 (820.02), 656.78 (656.22), 547.52 (547.01), 469.42 (469.01), 410.89 (410.51), 365.39 (365.01)
A9ValValA8	828.17 (827.03), 662.51 (661.82), 552.32 (551.69), 473.60 (473.02), 414.51 (414.02)
A9ValA9	820.88 (820.02), 656.90 (656.22), 547.58 (547.01), 469.55 (469.01), 410.95 (410.51)
A9AbuAbuA8	820.94, 656.90, 547.52, 469.48, 410.89, 365.39
A9AbuA9	817.20, 653.97, 545.15, 467.43, 409.08, 363.83
A9LeuLeuA8	835.03 (83), 668.12 (667.43), 556.87 (556.36), 477.46 (477.02), 417.94 (417.52)
A9LeuA9	824.25 (823.52), 659.52 (659.02), 549.76 (549.35), 471.42 (471.02), 412.57 (412.26)
A9IleIleA8	835.03 (834.03), 668.25 (667.43), 556.99 (556.36), 477.59 (477.02), 418.06 (417.52)
A9IleA9	824.18 (823.52), 659.46 (659.02), 549.70 (549.35), 471.29 (471.02), 412.51 (412.26)

A9MetMetA8	843.69 (843.01), 675.10 (674.61), 562.79 (562.34), 482.51 (482.15), 422.30 (422.01)
A9MetA9	828.79 (828.01), 663.26 (662.61), 552.88 (552.34), 474.03 (473.58), 414.94 (414.51)
A9PhePheA8	681.33 (681.02), 567.92 (567.69), 486.96 (486.73), 426.27 (426.02)
A9PheA9	666.69 (665.82), 555.62 (555.01), 476.46 (475.87), 417.06 (416.51)
A9TyrTyrA8	687.56 (687.42), 573.02 (573.14), 491.43 (491.30), 430.10 (430.02)
A9TyrA9	836.76 (836.02), 669.71 (669.01), 558.13 (557.68), 478.56 (478.16), 418.88 (418.51)
A9AsnAsnA8	556.93 (556.68), 477.46 (477.30), 417.94 (417.76)
A9AsnA9	659.71 (659.21), 549.89 (549.51), 471.42 (471.15), 412.64 (412.38)
A9SerSerA8	657.59 (657.01), 548.14 (547.67), 469.98 (469.58), 411.39 (411.01)
A9SerA9	654.22 (653.81), 545.29 (545.01), 467.49 (467.29), 409.20 (409.01)
A9ThrThrA8	552.82 (552.35), 473.97 (473.58), 414.88 (414.51)
A9ThrA9	820.79 (820.51), 656.83 (656.61), 547.53 (547.34), 469.41(469.30), 410.86 (410.76)
A9GlnGlnA8	673.79 (673.42), 561.65 (561.35), 481.58 (481.30), 421.51 (421.26)
A9GlnA9	551.94 (551.85), 473.22 (473.15)
A9GlyGlyA8	806.57 (806.00), 645.44 (645.00), 538.10 (537.67), 461.37 (461.00), 403.83 (403.50)
A9GlyA9	648.43 (647.81), 540.64 (540.01), 463.53 (463.01), 405.75 (405.26)
A9ProA9	820.03 (819.51), 656.26 (655.81), 547.02 (546.68), 468.97 (468.73), 410.55 (410.26)
LysA18	552.26 (551.85), 473.53 (473.16), 414.38 (414.14)
ALysA17	552.26 (551.85), 473.53 (473.16), 414.44 (414.14)
A2LysA16	662.07 (662.02), 551.95 (551.85), 473.13 (473.16), 414.21 (414.14)
A3LysA15	552.32 (551.85), 473.66 (473.16), 414.57 (414.14)
HisA18	829.95 (829.51), 664.21 (663.81), 553.65 (553.35), 474.71 (474.44), 415.47 (415.26)
A4HisA14	829.76 (829.51), 664.03 (663.81), 553.46 (553.35), 474.52 (474.44), 415.41 (415.26)

A9HisA9	830.01 (829.51), 664.15 (663.81), 553.59 (553.35), 474.71 (474.44), 415.54 (415.26)
A12HisA6	829.69 (829.51), 663.90 (663.81), 553.46 (553.35), 474.52 (474.44), 415.28 (415.26)
A15HisA3	829.76 (829.51), 664.09 (663.81), 553.52 (553.35), 474.59 (474.44), 415.41 (415.26)
A18His	830.20 (829.51), 664.40 (663.81), 553.78 (553.35), 474.84 (474.44), 415.60 (415.26)
A9HisHisA8	846.51 (846.02), 677.48 (677.02), 564.71 (564.35), 484.23 (483.87), 423.87 (423.51), 376.92 (376.57)
ArgA18	834.87 (834.28), 668.13 (667.62), 556.93 (556.52), 477.55 (477.16)
A4ArgA14	834.93 (834.28), 668.13 (667.62), 556.93 (556.52), 477.55 (477.16)
A9ArgA9	667.753 (667.62), 556.62 (556.52), 477.24 (477.16), 417.68 (417.64)
A12ArgA6	834.87 (834.28), 668.07 (667.62), 556.93 (556.52), 477.55 (477.16)
A15ArgA3	834.49 (834.28), 667.75 (667.62), 556.56 (556.52), 477.24 (477.16), 417.68 (417.64)
A18Arg	834.49 (834.28), 667.88 (667.62), 556.68 (556.52), 477.37 (477.16), 417.81 (417.64)
A9ArgArgA8	685.18 (684.63), 571.08 (570.70), 489.68 (489.31), 428.61 (428.27)
A9AspAspA8	835.82 (835.00), 668.82 (668.21), 557.57 (557.01), 478.06 (477.58),
A9AspA9	824.83 (824.01), 660.05 (659.41), 550.18 (549.67), 471.81 (471.29)
A9GluGluA8	842.76 (842.01), 674.38 (673.81), 562.18 (561.68), 482.04 (481.58), 421.91 (421.51)
A9GluA9	828.30 (827.51), 662.89 (662.21), 552.51 (552.01), 473.77 (473.30), 414.65 (414.26)
A9S(OMe)S(OMe)A8	828.88 (828.01), 663.32 (662.61), 552.82 (552.35), 474.17 (473.58), 415.05 (414.51)
A9S(OMe)A9	821.05 (820.51), 656.99 (656.61), 547.70 (547.34), 469.58 (469.30), 411.08 (410.76)

### III. $^{13}\text{C}=\text{O}$ NMR-derived Data and MS Data for Series 1 Peptides

**Table 1.** Helical propensities assigned from  $^{13}\text{C}=\text{O}$  chemical shifts in  $^t\text{L}\text{-Ala}_9\text{-Xxx-Ala}_9\text{-tL}$  at  $2^\circ\text{C}$ .

Amino Acid	Helical Propensity at $T = 2^\circ\text{C}$		$^{13}\text{C}=\text{O}$ Chemical Shift		
	$\emptyset w_{\text{XXX}}$	SD	Site 12	Site 14	Site 15
Ala	1.56	-	180.576	180.261	179.995
Nle	1.49	0.06	180.563	180.261	179.986
Nva	1.47	0.05	180.564	180.287	179.991
Glu	1.22	0.21	180.476	180.247	179.947
Leu	1.10	0.20	180.448	180.229	179.926
Arg	0.87	0.04	180.435	180.123	179.881
Met	0.87	0.06	180.398	180.142	179.885
Ile	0.78	0.02	180.389	180.087	179.858
Gln	0.68	0.07	180.288	180.082	179.826
Lys	0.67	0.06	180.357	180.036	179.807
Asp	0.56	0.04	180.247	180.000	179.757
Val	0.55	0.02	180.242	179.981	179.757
Trp	0.53	0.08	180.142	180.005	179.752
Phe	0.52	0.08	180.146	180.004	179.734
Tyr	0.50	0.09	180.105	180.000	179.716
Ser	0.45	0.07	180.151	179.931	179.633
Asn	0.37	0.04	180.041	179.835	179.579
Cys	0.37	0.02	180.032	179.821	179.611
Thr	0.36	0.02	180.050	179.817	-
His	0.18	0.02	179.624	179.441	179.258
Gly	0.17	0.02	179.592	179.377	179.212
Pro	0.013	0.004	178.237	179.201	178.324

**Table 2.** Helical propensities assigned from  $^{13}\text{C}=\text{O}$  chemical shifts in  $^t\text{L}\text{-Ala}_9\text{-Xxx-Ala}_9\text{-tL}$  at  $25^\circ\text{C}$ .

Amino Acid	Helical Propensity at $T = 25^\circ\text{C}$		$^{13}\text{C}=\text{O}$ Chemical Shift		
	$\emptyset w_{\text{XXX}}$	SD	Site 12	Site 14	Site 15
Ala	1.39	-	179.734	179.391	179.144
Nle	1.37	0.06	179.707	179.405	179.139
Nva	1.20	0.05	179.643	179.350	179.098
Leu	1.15	0.10	179.597	179.354	179.079
Glu	1.00	0.07	179.546	179.290	179.015
Met	0.90	0.03	179.473	179.221	178.997
Ile	0.81	0.03	179.418	179.176	178.956
Arg	0.80	0.04	179.450	179.153	178.933
Gln	0.72	0.03	179.327	179.121	178.906
Trp	0.64	0.07	179.208	179.089	178.851
Lys	0.60	0.04	179.276	179.006	178.814
Asp	0.54	0.03	179.199	178.965	178.764
Val	0.53	0.03	179.162	178.970	178.764
Ser	0.51	0.03	179.144	178.951	178.732
Phe	0.50	0.04	179.075	178.960	178.754
Tyr	0.50	0.04	179.066	178.965	178.750
Asn	0.43	0.04	179.038	178.846	178.663
Thr	0.40	0.02	178.988	178.823	-
Cys	0.36	0.01	178.892	178.759	178.608
Gly	0.22	0.02	178.613	178.471	178.361
His	0.20	0.02	178.562	178.448	178.324
Pro	0.045	0.01	177.949	177.926	177.972

**Table 3. Helical propensities assigned from  $^{13}\text{C}=\text{O}$  chemical shifts in  ${}^t\text{L-Ala}_9\text{-Xxx-Ala}_9\text{-}{}^t\text{L}$  at 60°C.**

Amino Acid	Helical Propensity at $T = 60^\circ\text{C}$		$^{13}\text{C}=\text{O}$ Chemical Shift		
	$\emptyset w_{XXX}$	SD	Site 12	Site 14	Site 15
Nle	1.24	0.04	178.178	178.026	177.889
Leu	1.22	0.05	178.159	178.022	177.885
Ala	1.17	-	178.159	177.999	177.857
Nva	1.14	0.03	178.127	177.985	177.857
Glu	1.04	0.01	178.086	177.949	177.817
Met	0.99	0.04	178.036	177.921	177.816
Ile	0.98	0.05	178.017	177.917	177.811
Asp	0.94	0.03	178.045	177.875	177.770
Trp	0.92	0.07	177.962	177.903	177.793
Gln	0.86	0.04	177.958	177.866	177.766
Ser	0.83	0.03	177.944	177.848	177.752
Val	0.78	0.04	177.894	177.834	177.734
Asn	0.75	0.05	177.926	177.784	177.720
Tyr	0.72	0.06	177.830	177.811	177.715
Phe	0.72	0.06	177.830	177.807	177.715
Thr	0.71	0.02	177.848	177.788	-
Arg	0.70	0.03	177.880	177.770	177.688
Lys	0.67	0.02	177.853	177.756	177.679
Cys	0.59	0.03	177.734	177.734	177.660
Gly	0.51	0.02	177.724	177.660	177.614
Pro	0.31	0.03	177.541	177.541	177.541
His	0.31	0.01	177.546	178.546	177.509

**Table 4.** Relative free energies with standard deviations for the twenty naturally occurring amino acids plus norleucine and norvaline measured in <sup>t</sup>L-Ala<sub>9</sub>-Xxx-Ala<sub>9</sub>-<sup>t</sup>L, covering the temperature range of 2, 25, and 60°C.

Amino Acid	<i>T</i> = 2 °C		<i>T</i> = 25 °C		<i>T</i> = 60 °C	
	<i>ΔΔG</i>	<i>SD</i>	<i>ΔΔG</i>	<i>SD</i>	<i>ΔΔG</i>	<i>SD</i>
Ala	0.00	0.00	0.00	0.00	0.00	0.00
Nle	0.02	0.02	0.01	0.03	-0.04	0.02
Nva	0.03	0.02	0.09	0.03	0.02	0.02
Glu	0.14	0.09	0.19	0.04	0.08	0.00
Leu	0.19	0.09	0.11	0.05	-0.03	0.03
Arg	0.32	0.03	0.33	0.03	0.34	0.03
Met	0.32	0.04	0.26	0.02	0.11	0.03
Ile	0.38	0.02	0.32	0.02	0.12	0.04
Gln	0.45	0.06	0.39	0.03	0.20	0.03
Lys	0.46	0.05	0.50	0.03	0.37	0.02
Asp	0.56	0.04	0.56	0.04	0.15	0.02
Val	0.57	0.02	0.57	0.03	0.26	0.04
Trp	0.59	0.08	0.46	0.06	0.16	0.05
Phe	0.60	0.08	0.60	0.05	0.33	0.06
Tyr	0.63	0.10	0.60	0.05	0.30	0.06
Ser	0.69	0.09	0.59	0.04	0.23	0.02
Asn	0.79	0.07	0.69	0.03	0.29	0.05
Cys	0.78	0.03	0.79	0.02	0.46	0.06
Thr	0.79	0.06	0.74	0.06	0.33	0.04
His	1.17	0.06	1.16	0.06	0.88	0.02
Gly	1.22	0.06	1.10	0.05	0.55	0.04
Pro	2.63	0.18	2.03	0.13	0.85	0.09

**Table 5. Chemical Shift Scan at 2, 25, and 60°C for the Series of Hydrophobic Guests in Ala<sub>19</sub>: W-K<sub>6</sub>-<sup>t</sup>L<sub>3</sub>-A<sub>9</sub>-Xxx-A<sub>9</sub>-<sup>t</sup>L<sub>3</sub>-K<sub>6</sub>-NH<sub>2</sub>; Xxx = Ala, Nva, Val**

Site <sup>13</sup> C=O Label	Chemical shift (ppm) measured at the Indicated Temperature								
	Ala			Nva			Val		
	2°C	25°C	60°C	2°C	25°C	60°C	2°C	25°C	60°C
1	178.109	177.656	176.969	178.091	177.619	176.928	178.013	177.500	176.910
2	179.597	178.722	177.560	179.580	178.640	177.514	179.221	178.278	177.408
3	179.817	178.960	177.697	179.859	178.878	177.669	179.441	178.452	177.518
4	180.224	179.258	177.862	180.151	179.121	177.775	179.743	178.649	177.614
5	180.499	179.537	177.999	180.385	179.372	177.917	179.899	178.773	177.651
6	180.590	179.675	178.086	180.325	179.372	177.949	179.569	178.645	177.660
7	180.654	179.771	178.168	180.710	179.752	178.159	180.384	179.153	177.766
8	180.709	179.844	178.210	180.499	179.643	178.127	179.977	178.970	177.729
9	180.723	179.885	178.242	180.755	179.913	178.315	180.650	179.459	178.063
10	180.705	179.881	178.228	180.302	180.421	-	180.302	179.176	177.802
11	180.673	179.821	178.223	180.242	180.316	Table 3	180.242	179.162	177.894
12	180.576	179.734	178.159	180.045	180.132	-	180.045	179.038	177.871
14	180.261	179.391	177.999	179.981	180.004	Table 3	179.981	178.970	177.834
15	179.995	179.144	177.857	179.757	179.739	Table 3	179.757	178.764	177.734
17	178.384	177.903	177.267	179.359	179.327	-	179.359	178.471	177.587
18	177.702	177.473	177.088	178.301	178.237	-	178.301	177.775	177.221
19	177.477	177.340	177.051	177.683	177.633	-	177.683	177.418	177.065

**Table 6. Chemical Shift Scan at 2, 25, and 60°C for the Series of Hydrophobic Guests in Ala<sub>19</sub>: W-K<sub>6</sub>-<sup>t</sup>L<sub>3</sub>-A<sub>9</sub>-Xxx-A<sub>9</sub>-<sup>t</sup>L<sub>3</sub>-K<sub>6</sub>-NH<sub>2</sub>; Xxx = Leu, Nle, Ile**

Site <sup>13</sup> C=O Label	Chemical shift (ppm) measured at the Indicated Temperature								
	Leu			Nle			Ile		
	2°C	25°C	60°C	2°C	25°C	60°C	2°C	25°C	60°C
1	178.095	177.628	176.960	178.114	177.656	176.969	177.990	177.518	176.891
2	179.473	178.594	177.509	179.542	178.658	177.523	179.272	178.420	177.431
3	179.743	178.823	177.665	179.807	178.906	177.697	179.510	178.567	177.540
4	180.087	179.116	177.834	180.183	179.208	177.848	179.826	178.809	177.656
5	180.279	179.295	177.930	180.407	179.441	177.976	180.018	179.020	177.756
6	180.206	179.258	177.949	180.384	179.423	177.990	179.858	178.864	177.729
7	180.728	179.844	178.297	180.696	179.826	178.232	180.522	179.459	177.917
8	180.467	179.638	178.205	180.549	179.716	178.182	180.160	179.263	177.875
9	180.934	180.027	178.406	180.810	180.027	178.411	180.824	179.748	178.168
10	180.609	179.720	178.168	180.663	179.784	178.173	180.430	179.455	177.917
11	180.448	179.597	178.159	180.563	179.707	178.178	180.389	179.418	178.017
12	180.302	179.464	178.100	180.375	179.546	178.113	180.174	179.276	177.985
14	180.229	179.354	178.022	180.261	179.405	178.026	180.087	179.176	177.917
15	179.926	179.079	177.885	179.986	179.139	177.889	179.858	178.956	177.811
17	179.519	178.718	177.701	179.583	178.777	177.701	179.492	178.635	177.642
18	178.356	177.894	177.276	178.393	177.917	177.280	178.338	177.853	177.253
19	177.702	177.473	177.102	177.711	177.477	177.097	177.702	177.459	177.083

**Table 7.  $^{13}\text{C}=\text{O}$  Labeling and Mass Spec Data for  $^t\text{L}_3\text{-A}_9\text{-Xxx-A}_9\text{-}^t\text{L}_3$ ; Xxx = 20 Natural Amino Acids plus Nle, Nva**

Note: Every peptide synthesized in this study was C-terminally amidated.

Peptide Sequence	Site $^{13}\text{C}=\text{O}$ Label	Percent $^{13}\text{C}=\text{O}$ Label	Average MW (Da)	$[m+zH]/z$ Expected					$[m+zH]/z$ Observed				
				4	5	6	7	8	4	5	6	7	8
<i>Xxx = 20 Natural Amino Acids plus Nle, Nva</i>													
W-K <sub>6</sub> - <sup>t</sup> L <sub>3</sub> -A <sub>9</sub> -A-A <sub>9</sub> - <sup>t</sup> L <sub>3</sub> -K <sub>6</sub>	12,14,15	100/75/50	3772.78	943.62	755.10	629.42	539.64	472.31	944.00	756.00	630.00	540.00	472.00
W-K <sub>6</sub> - <sup>t</sup> L <sub>3</sub> -A <sub>9</sub> -C-A <sub>9</sub> - <sup>t</sup> L <sub>3</sub> -K <sub>6</sub>	12,14,15	100/75/50	3804.84	951.61	761.49	634.74	544.21	476.31	952.00	762.00	635.00	544.00	476.00
W-K <sub>6</sub> - <sup>t</sup> L <sub>3</sub> -A <sub>9</sub> -D-A <sub>9</sub> - <sup>t</sup> L <sub>3</sub> -K <sub>6</sub>	12,14,15	100/75/50	3816.79	954.62	763.90	636.75	545.93	477.81	955.00	764.00	637.00	546.00	478.00
W-K <sub>6</sub> - <sup>t</sup> L <sub>3</sub> -A <sub>9</sub> -E-A <sub>9</sub> - <sup>t</sup> L <sub>3</sub> -K <sub>6</sub>	12,14,15	100/75/50	3830.81	958.12	766.70	639.08	547.93	479.56	959.00	767.00	639.00	548.00	480.00
W-K <sub>6</sub> - <sup>t</sup> L <sub>3</sub> -A <sub>9</sub> -F-A <sub>9</sub> - <sup>t</sup> L <sub>3</sub> -K <sub>6</sub>	12,14,15	100/75/50	3848.87	962.63	770.30	642.09	550.51	481.82	963.00	771.00	643.00	551.00	482.00
W-K <sub>6</sub> - <sup>t</sup> L <sub>3</sub> -A <sub>9</sub> -G-A <sub>9</sub> - <sup>t</sup> L <sub>3</sub> -K <sub>6</sub>	12,14,15	100/75/50	3758.75	940.12	752.29	627.08	537.64	470.56	940.00	753.00	627.00	538.00	471.00
W-K <sub>6</sub> - <sup>t</sup> L <sub>3</sub> -A <sub>9</sub> -H-A <sub>9</sub> - <sup>t</sup> L <sub>3</sub> -K <sub>6</sub>	12,14,15	100/75/50	3838.84	960.13	768.30	640.42	549.08	480.57	961.00	768.00	641.00	550.00	481.00
W-K <sub>6</sub> - <sup>t</sup> L <sub>3</sub> -A <sub>9</sub> -I-A <sub>9</sub> - <sup>t</sup> L <sub>3</sub> -K <sub>6</sub>	12,14,15	100/75/50	3814.86	954.13	763.51	636.42	545.65	477.57	955.00	764.00	637.00	546.00	478.00
W-K <sub>6</sub> - <sup>t</sup> L <sub>3</sub> -A <sub>9</sub> -K-A <sub>9</sub> - <sup>t</sup> L <sub>3</sub> -K <sub>6</sub>	12,14,15	100/75/50	3829.87	957.88	766.51	683.93	547.79	479.45	958.00	767.00	640.00	548.00	480.00
W-K <sub>6</sub> - <sup>t</sup> L <sub>3</sub> -A <sub>9</sub> -L-A <sub>9</sub> - <sup>t</sup> L <sub>3</sub> -K <sub>6</sub>	12,14,15	100/75/50	3814.86	954.13	763.51	636.42	545.65	477.57	954.00	764.00	636.00	546.00	478.00
W-K <sub>6</sub> - <sup>t</sup> L <sub>3</sub> -A <sub>9</sub> -M-A <sub>9</sub> - <sup>t</sup> L <sub>3</sub> -K <sub>6</sub>	12,14,15	100/75/50	3832.90	958.62	767.10	639.42	548.22	479.81	959.00	767.00	640.00	549.00	480.00
W-K <sub>6</sub> - <sup>t</sup> L <sub>3</sub> -A <sub>9</sub> -N-A <sub>9</sub> - <sup>t</sup> L <sub>3</sub> -K <sub>6</sub>	12,14,15	100/75/50	3815.80	954.37	763.70	636.58	545.79	477.69	955.00	764.00	637.00	546.00	478.00
W-K <sub>6</sub> - <sup>t</sup> L <sub>3</sub> -A <sub>9</sub> -P-A <sub>9</sub> - <sup>t</sup> L <sub>3</sub> -K <sub>6</sub>	12,14,15	100/75/50	3798.81	950.12	760.30	633.75	543.36	475.57	951.00	761.00	634.00	544.00	476.00
W-K <sub>6</sub> - <sup>t</sup> L <sub>3</sub> -A <sub>9</sub> -Q-A <sub>9</sub> - <sup>t</sup> L <sub>3</sub> -K <sub>6</sub>	12,14,15	100/75/50	3829.83	957.88	766.50	638.92	547.79	479.44	958.00	767.00	639.00	548.00	479.00
W-K <sub>6</sub> - <sup>t</sup> L <sub>3</sub> -A <sub>9</sub> -R-A <sub>9</sub> - <sup>t</sup> L <sub>3</sub> -K <sub>6</sub>	12,14,15	100/75/50	3857.88	964.89	772.11	643.59	551.80	482.95	965.00	772.00	644.00	552.00	483.00
W-K <sub>6</sub> - <sup>t</sup> L <sub>3</sub> -A <sub>9</sub> -S-A <sub>9</sub> - <sup>t</sup> L <sub>3</sub> -K <sub>6</sub>	12,14,15	100/75/50	3788.78	947.62	758.30	632.08	541.93	474.31	948.00	758.00	632.00	542.00	475.00
W-K <sub>6</sub> - <sup>t</sup> L <sub>3</sub> -A <sub>9</sub> -T-A <sub>9</sub> - <sup>t</sup> L <sub>3</sub> -K <sub>6</sub>	12,14,16	100/75/50	3802.80	951.12	761.10	634.42	543.93	476.07	951.00	761.00	635.00	544.00	477.00
W-K <sub>6</sub> - <sup>t</sup> L <sub>3</sub> -A <sub>9</sub> -V-A <sub>9</sub> - <sup>t</sup> L <sub>3</sub> -K <sub>6</sub>	12,14,15	100/75/50	3800.83	950.63	760.70	634.09	543.65	475.82	951.00	761.00	634.00	544.00	476.00
W-K <sub>6</sub> - <sup>t</sup> L <sub>3</sub> -A <sub>9</sub> -W-A <sub>9</sub> - <sup>t</sup> L <sub>3</sub> -K <sub>6</sub>	12,14,15	100/75/50	3887.91	972.38	778.11	648.59	556.08	486.69	972.00	778.00	649.00	556.00	487.00
W-K <sub>6</sub> - <sup>t</sup> L <sub>3</sub> -A <sub>9</sub> -Y-A <sub>9</sub> - <sup>t</sup> L <sub>3</sub> -K <sub>6</sub>	12,14,15	100/75/50	3864.87	966.63	773.50	644.75	552.79	483.82	967.00	774.00	645.00	553.00	484.00
W-K <sub>6</sub> - <sup>t</sup> L <sub>3</sub> -A <sub>9</sub> -Nle-A <sub>9</sub> - <sup>t</sup> L <sub>3</sub> -K <sub>6</sub>	12,14,15	100/75/50	3814.86	954.13	763.51	636.42	545.65	477.57	955.00	764.00	637.00	545.00	478.00
W-K <sub>6</sub> - <sup>t</sup> L <sub>3</sub> -A <sub>9</sub> -Nva-A <sub>9</sub> - <sup>t</sup> L <sub>3</sub> -K <sub>6</sub>	12,14,15	100/75/50	3800.83	950.63	760.70	634.09	543.65	475.82	951.00	761.00	635.00	544.00	476.00

**Table 8.  $^{13}\text{C}=\text{O}$  Labeling and Mass Spec Data for Chemical Shift Scans of  $^t\text{L}_3\text{-A}_9\text{-Xxx-A}_9\text{-}^t\text{L}_3$ ; Xxx = Ala, Ile**

Note: Every peptide synthesized in this study was C-terminally amidated.

Peptide Sequence	Site $^{13}\text{C}=\text{O}$ Label	Percent $^{13}\text{C}=\text{O}$ Label	Average MW (Da)	$[m+zH]/z$ Expected					$[m+zH]/z$ Observed				
				4	5	6	7	8	4	5	6	7	8
<i>Xxx = Ala</i>													
W-K <sub>6</sub> - <sup>t</sup> L <sub>3</sub> -A <sub>9</sub> -A-A <sub>9</sub> - <sup>t</sup> L <sub>3</sub> -K <sub>6</sub>	1,4,7	100/80/60	3772.78	943.62	755.10	629.42	539.64	472.31	944.00	756.00	630.00	540.00	472.00
W-K <sub>6</sub> - <sup>t</sup> L <sub>3</sub> -A <sub>9</sub> -A-A <sub>9</sub> - <sup>t</sup> L <sub>3</sub> -K <sub>6</sub>	2,5,8	25/50/100	3772.78	943.62	755.10	629.42	539.64	472.31	944.00	756.00	630.00	540.00	472.00
W-K <sub>6</sub> - <sup>t</sup> L <sub>3</sub> -A <sub>9</sub> -A-A <sub>9</sub> - <sup>t</sup> L <sub>3</sub> -K <sub>6</sub>	3,6,9	25/50/100	3772.78	943.62	755.10	629.42	539.64	472.31	944.00	756.00	630.00	540.00	472.00
W-K <sub>6</sub> - <sup>t</sup> L <sub>3</sub> -A <sub>9</sub> -A-A <sub>9</sub> - <sup>t</sup> L <sub>3</sub> -K <sub>6</sub>	3,10,19	25/50/100	3772.78	943.62	755.10	629.42	539.64	472.31	944.00	756.00	630.00	540.00	472.00
W-K <sub>6</sub> - <sup>t</sup> L <sub>3</sub> -A <sub>9</sub> -A-A <sub>9</sub> - <sup>t</sup> L <sub>3</sub> -K <sub>6</sub>	11,14,17	25/50/100	3772.78	943.62	755.10	629.42	539.64	472.31	944.00	756.00	630.00	540.00	472.00
W-K <sub>6</sub> - <sup>t</sup> L <sub>3</sub> -A <sub>9</sub> -A-A <sub>9</sub> - <sup>t</sup> L <sub>3</sub> -K <sub>6</sub>	12,15,18	25/50/100	3772.78	943.62	755.10	629.42	539.64	472.31	944.00	756.00	630.00	540.00	472.00
W-K <sub>6</sub> - <sup>t</sup> L <sub>3</sub> -A <sub>9</sub> -A-A <sub>9</sub> - <sup>t</sup> L <sub>3</sub> -K <sub>6</sub>	13,15,17	25/50/100	3772.78	943.62	755.10	629.42	539.64	472.31	944.00	756.00	630.00	540.00	472.00
<i>Xxx = Ile</i>													
W-K <sub>6</sub> - <sup>t</sup> L <sub>3</sub> -A <sub>9</sub> -I-A <sub>9</sub> - <sup>t</sup> L <sub>3</sub> -K <sub>6</sub>	1,4,7	25/50/100	3814.86	954.13	763.51	636.42	545.65	477.57	955.00	764.00	637.00	546.00	478.00
W-K <sub>6</sub> - <sup>t</sup> L <sub>3</sub> -A <sub>9</sub> -I-A <sub>9</sub> - <sup>t</sup> L <sub>3</sub> -K <sub>6</sub>	2,5,8	25/50/100	3814.86	954.13	763.51	636.42	545.65	477.57	955.00	764.00	637.00	546.00	478.00
W-K <sub>6</sub> - <sup>t</sup> L <sub>3</sub> -A <sub>9</sub> -I-A <sub>9</sub> - <sup>t</sup> L <sub>3</sub> -K <sub>6</sub>	3,6,9	25/50/100	3814.86	954.13	763.51	636.42	545.65	477.57	955.00	764.00	637.00	546.00	478.00
W-K <sub>6</sub> - <sup>t</sup> L <sub>3</sub> -A <sub>9</sub> -I-A <sub>9</sub> - <sup>t</sup> L <sub>3</sub> -K <sub>6</sub>	11,14,17	25/50/100	3814.86	954.13	763.51	636.42	545.65	477.57	955.00	764.00	637.00	546.00	478.00
W-K <sub>6</sub> - <sup>t</sup> L <sub>3</sub> -A <sub>9</sub> -I-A <sub>9</sub> - <sup>t</sup> L <sub>3</sub> -K <sub>6</sub>	12,15,18	25/50/100	3814.86	954.13	763.51	636.42	545.65	477.57	955.00	764.00	637.00	546.00	478.00
W-K <sub>6</sub> - <sup>t</sup> L <sub>3</sub> -A <sub>9</sub> -I-A <sub>9</sub> - <sup>t</sup> L <sub>3</sub> -K <sub>6</sub>	13,16,19	25/50/100	3814.86	954.13	763.51	636.42	545.65	477.57	955.00	764.00	637.00	546.00	478.00

**Table 9.  $^{13}\text{C}=\text{O}$  Labeling and Mass Spec Data for Chemical Shift Scans of  $^t\text{L}_3\text{-A}_9\text{-Xxx-A}_9\text{-}^t\text{L}_3$ ; Xxx = Leu, Nle, Nva, Val**

Note: Every peptide synthesized in this study was C-terminally amidated.

Peptide Sequence	Site $^{13}\text{C}=\text{O}$ Label	Percent $^{13}\text{C}=\text{O}$ Label	Average MW (Da)	$[m+zH]/z$ Expected					$[m+zH]/z$ Observed				
				4	5	6	7	8	4	5	6	7	8
<i>Xxx = Leu</i>													
W-K <sub>6</sub> - <sup>t</sup> L <sub>3</sub> -A <sub>9</sub> -L-A <sub>9</sub> - <sup>t</sup> L <sub>3</sub> -K <sub>6</sub>	1,4,7	25/50/100	3814.86	954.13	763.51	636.42	545.65	477.57	954.00	764.00	637.00	546.00	478.00
W-K <sub>6</sub> - <sup>t</sup> L <sub>3</sub> -A <sub>9</sub> -L-A <sub>9</sub> - <sup>t</sup> L <sub>3</sub> -K <sub>6</sub>	2,5,8	25/50/100	3814.86	954.13	763.51	636.42	545.65	477.57	954.00	764.00	637.00	546.00	478.00
W-K <sub>6</sub> - <sup>t</sup> L <sub>3</sub> -A <sub>9</sub> -L-A <sub>9</sub> - <sup>t</sup> L <sub>3</sub> -K <sub>6</sub>	3,6,9	25/50/100	3814.86	954.13	763.51	636.42	545.65	477.57	954.00	764.00	637.00	546.00	478.00
W-K <sub>6</sub> - <sup>t</sup> L <sub>3</sub> -A <sub>9</sub> -L-A <sub>9</sub> - <sup>t</sup> L <sub>3</sub> -K <sub>6</sub>	11,14,17	25/50/100	3814.86	954.13	763.51	636.42	545.65	477.57	954.00	764.00	637.00	546.00	478.00
W-K <sub>6</sub> - <sup>t</sup> L <sub>3</sub> -A <sub>9</sub> -L-A <sub>9</sub> - <sup>t</sup> L <sub>3</sub> -K <sub>6</sub>	12,15,18	25/50/100	3814.86	954.13	763.51	636.42	545.65	477.57	954.00	764.00	637.00	546.00	478.00
W-K <sub>6</sub> - <sup>t</sup> L <sub>3</sub> -A <sub>9</sub> -L-A <sub>9</sub> - <sup>t</sup> L <sub>3</sub> -K <sub>6</sub>	13,16,19	25/50/100	3814.86	954.13	763.51	636.42	545.65	477.57	954.00	764.00	637.00	546.00	478.00
<i>Xxx = Nle</i>													
W-K <sub>6</sub> - <sup>t</sup> L <sub>3</sub> -A <sub>9</sub> -Nle-A <sub>9</sub> - <sup>t</sup> L <sub>3</sub> -K <sub>6</sub>	1,3,5,7,9	20/40/60/80/100	3816.86	954.63	763.91	636.76	545.94	477.82	955.00	764.00	637.00	546.00	478.00
W-K <sub>6</sub> - <sup>t</sup> L <sub>3</sub> -A <sub>9</sub> -Nle-A <sub>9</sub> - <sup>t</sup> L <sub>3</sub> -K <sub>6</sub>	2,4,6,8	25/50/75/100	3815.85	954.38	763.71	636.59	545.79	477.70	954.00	764.00	637.00	546.00	478.00
W-K <sub>6</sub> - <sup>t</sup> L <sub>3</sub> -A <sub>9</sub> -Nle-A <sub>9</sub> - <sup>t</sup> L <sub>3</sub> -K <sub>6</sub>	12,14,16,18	25/50/75/100	3815.85	954.38	763.71	636.59	545.79	477.70	954.00	764.00	637.00	546.00	478.00
W-K <sub>6</sub> - <sup>t</sup> L <sub>3</sub> -A <sub>9</sub> -Nle-A <sub>9</sub> - <sup>t</sup> L <sub>3</sub> -K <sub>6</sub>	11,13,15,17,19	20/40/60/80/100	3816.86	954.63	763.91	636.76	545.94	477.82	955.00	764.00	637.00	546.00	478.00
<i>Xxx = Nva</i>													
W-K <sub>6</sub> - <sup>t</sup> L <sub>3</sub> -A <sub>9</sub> -Nva-A <sub>9</sub> - <sup>t</sup> L <sub>3</sub> -K <sub>6</sub>	1,4,9	25/50/100	3800.83	950.63	760.70	634.09	543.65	475.82	951.00	761.00	634.00	544.00	476.00
W-K <sub>6</sub> - <sup>t</sup> L <sub>3</sub> -A <sub>9</sub> -Nva-A <sub>9</sub> - <sup>t</sup> L <sub>3</sub> -K <sub>6</sub>	2,4,6,8	25/50/75/100	3801.83	950.88	760.90	634.26	543.79	475.94	951.00	761.00	635.00	544.00	476.00
W-K <sub>6</sub> - <sup>t</sup> L <sub>3</sub> -A <sub>9</sub> -Nva-A <sub>9</sub> - <sup>t</sup> L <sub>3</sub> -K <sub>6</sub>	2,3,5,6,7	20/40/60/80/100	3802.84	951.13	761.11	634.42	543.93	476.07	952.00	761.00	634.00	544.00	476.00
W-K <sub>6</sub> - <sup>t</sup> L <sub>3</sub> -A <sub>9</sub> -Nva-A <sub>9</sub> - <sup>t</sup> L <sub>3</sub> -K <sub>6</sub>	8,12,14,16,18	20/40/60/80/100	3802.84	951.13	761.11	634.42	543.93	476.07	952.00	761.00	634.00	544.00	476.00
W-K <sub>6</sub> - <sup>t</sup> L <sub>3</sub> -A <sub>9</sub> -Nva-A <sub>9</sub> - <sup>t</sup> L <sub>3</sub> -K <sub>6</sub>	11,13,15,17,19	20/40/60/80/100	3802.84	951.13	761.11	634.42	543.93	476.07	952.00	761.00	634.00	544.00	476.00
<i>Xxx = Val</i>													
W-K <sub>6</sub> - <sup>t</sup> L <sub>3</sub> -A <sub>9</sub> -V-A <sub>9</sub> - <sup>t</sup> L <sub>3</sub> -K <sub>6</sub>	1,4,9	25/50/100	3800.83	950.63	760.70	634.09	543.65	475.82	951.00	761.00	634.00	544.00	476.00
W-K <sub>6</sub> - <sup>t</sup> L <sub>3</sub> -A <sub>9</sub> -V-A <sub>9</sub> - <sup>t</sup> L <sub>3</sub> -K <sub>6</sub>	2,4,6,8	25/50/75/100	3801.83	950.88	760.90	634.26	543.79	475.94	951.00	761.00	635.00	544.00	476.00
W-K <sub>6</sub> - <sup>t</sup> L <sub>3</sub> -A <sub>9</sub> -V-A <sub>9</sub> - <sup>t</sup> L <sub>3</sub> -K <sub>6</sub>	2,3,5,6,7	20/40/60/80/100	3802.84	951.13	761.11	634.42	543.93	476.07	952.00	761.00	634.00	544.00	476.00
W-K <sub>6</sub> - <sup>t</sup> L <sub>3</sub> -A <sub>9</sub> -V-A <sub>9</sub> - <sup>t</sup> L <sub>3</sub> -K <sub>6</sub>	8,12,14,16,18	20/40/60/80/100	3802.84	951.13	761.11	634.42	543.93	476.07	952.00	761.00	634.00	544.00	476.00
W-K <sub>6</sub> - <sup>t</sup> L <sub>3</sub> -A <sub>9</sub> -V-A <sub>9</sub> - <sup>t</sup> L <sub>3</sub> -K <sub>6</sub>	11,13,15,17,19	20/40/60/80/100	3802.84	951.13	761.11	634.42	543.93	476.07	952.00	761.00	634.00	544.00	476.00

**IV. CD ellipticities, which have corroborative value, are unsuited as primary tools for the assignment of helical propensities from host-guest mutants.**

A. Experimental circular dichroism characterization of helix-coil peptide equilibria; variability of helical structure; structural-dependences of the helical circular dichroism ellipticity  $[\theta]_{222,H,n,T}$

For a typical peptide the proximity-coupled  $\pi \rightarrow \pi^*$  and  $n \rightarrow \pi^*$  electronic and magnetic transitions of its backbone amides define the major CD chromophores within the wavelength region of 185 to 250 nm. Mean values of  $\phi$  and  $\psi$  dihedral angles, which fall within Ramachandran-allowed regions, define the signs and intensities of these transitions,<sup>1</sup> and for peptides in solution, CD ellipticities thus provide a unique tool for conformational assignments. The distinctive signature of the  $\alpha$ -helical conformation is an intense positive ellipticity maximum near 290 nm, and a pair of intense negative ellipticity minima at 208 and 222 nm.

$$[\theta]_{222,\text{Exper},n,T} = \text{FH} [\theta]_{222,H,n,T} + (1 - \text{FH}) [\theta]_{222,C,n,T} \quad (1)$$

$$[\theta]_{222,H,n,T} = [\theta]_{222,H,\infty,T} (1 - X/n) \quad 0 \leq X \leq 1.0 \quad (2)$$

With increasing temperature, a helical peptide in water that is unassociated and lacks stabilization from tertiary packing undergoes reversible helix-coil melting, characterized by a decrease in the mole fraction FH of its helical residues and a proportionate increase in the mole fraction (1 – FH) of residues that assume coil conformations. Given Equation (1) parameter values, one can to a good approximation characterize helix-coil melting from the experimental temperature dependence of the 222 nm molar per-residue ellipticity  $[\theta]_{222,\text{Exper},n,T}$ , and the accuracy of this two-state model can be confirmed for a particular peptide by ellipticities at 203 nm, at which coil and helix values are equal.<sup>2</sup> *The model is confirmed if the T-dependent CD spectra share a 203 nm isodichroic point.<sup>3</sup>* At one or more fixed temperatures, Equation (1) is also universally used to assign FH changes induced by a series of guest residue substitutions within a host helical peptide. However the single reported 203 nm test of the validity of this use failed to yield consistent isodichroic behavior.<sup>4</sup>

For either FH calculation, accurate assignments for the helicity parameters are essential, and the major issue explored in this supplement section is their accuracy when applied to host-guest data. Although the  $[\theta]_{222,H,n,T}$  and  $[\theta]_{222,H,\infty,T}$  parameters resemble UV-vis spectroscopic extinction coefficients, they differ in two fundamental respects: their intensities reflect the local structural environment, and they are temperature-sensitive.<sup>3,5,6</sup>

The structural variability of the  $\alpha$ -helix itself accounts for much of this sensitivity. An  $\alpha$ -helical conformation is defined by a contiguous sequence of backbone C=O to H-N amide hydrogen bonds of the 3.6<sub>13</sub> type, and modeling as well as examples from the PDB show this structural condition to be met provided the average of sums of  $\alpha$ -carbon  $\phi$ ,  $\psi$  pairs within the sequence lies close to  $-105^\circ$ .<sup>7</sup> However, within this constraint,  $\phi$  ranges from  $-25$  to  $-95^\circ$ , with corresponding  $\psi$  values of  $-80$  to  $-10^\circ$ .<sup>7</sup> Molecular modeling of polyalanines reveals the Ramachandran helical region as an extended  $\phi$ ,  $\psi$  trough, with shallow local minima, that spans these  $\phi$ ,  $\psi$  ranges.<sup>8</sup> Moreover ab initio CD modeling shows that this  $\alpha$ -helical  $\phi$ -angle variation results in a substantial intensity change for  $[\theta]_{222,H}$ ,<sup>9</sup> and experimental data support this prediction. Mean values for  $[\theta]_{222,H,\infty,T}$  of PDB  $\alpha$ -helices, which have a mean  $\phi$  of  $-63^\circ$ ,<sup>10</sup> fall within the range,  $-37 \times 10^3$  to  $-44 \times 10^3$  deg cm<sup>2</sup> dm<sup>-1</sup>, also consistent with length extrapolations from alanine-rich heteropeptide CD data.<sup>6</sup> A different picture emerges from our NMR and CD studies of core regions of N- and C-capped, fully helical polyalanine cores.<sup>11</sup> Their  $\phi$  is  $-51 \pm 2^\circ$ , close to an average of values for the classic fiber-diffraction structure and the Pauling  $\alpha$ -helix, and their  $[\theta]_{222,H,\infty,T}$  is  $-(60.5 \pm 1.3) \times 10^3$  deg cm<sup>2</sup> dm<sup>-1</sup>, confirmed by low temperature CD spectra of a winter flounder protein with a 70 % Ala content).<sup>12</sup>

The 3<sub>10</sub> helix, frequently detected within short helical regions of PDB globular proteins, is more tightly helical than the  $\alpha$ , with  $\phi = -49^\circ$ ,  $\psi = -25^\circ$ ,<sup>13</sup> and novel ESR<sup>14</sup> and NMR<sup>15</sup> structural methods, applied to a range of test peptides, demonstrate hybrid 3<sub>10</sub>- $\alpha$  character that is most pronounced within end regions. Peptides with pure 3<sub>10</sub> structure are characterized by exceptionally weak intensities for  $[\theta]_{222,H}$ , although shorter wavelength CD maxima and minima have nearly normal intensities.<sup>16</sup> Doubt clearly compromises accuracy for FH values assigned from  $[\theta]_{222,Exper}$  values of peptides that, like these, assume hybrid 3<sub>10</sub>- $\alpha$  structures.

B. Evidence for significant perturbations of the intensity of  $[\theta]_{222,H}$ : The end-region correction of Equation (2). Plausible corrections in  $[\theta]_{222,H,\infty,T}$  from <sup>13</sup>C=O NMR chemical shift data of mutants 1 and  $[\theta]_{\lambda,Exper,n,T}$  data of mutants 2; Tests of the validity of the two-state assumption of Equation (1) from  $[\theta]_{203}$  data. In the accompanying manuscript we report a set of temperature-dependent relative helical propensities  $w_{Xxx}/w_{Ala}$  assigned from  $[\theta]_{222,Exper,n,T}$  data for a mutant series 2 and a second propensity set assigned from <sup>13</sup>C=O NMR chemical shifts for a mutant series 1. Although statistical tests yield satisfactory correlations for this  $w_{Xxx}/w_{Ala}$  pair, the magnitudes for many of the ellipticity-derived  $w_{Xxx}/w_{Ala}$  are smaller than those derived from shifts. We now make the case that the likely

cause is a reduction in the intensity of  $[\theta]_{222,H,\infty,T}$ , caused by central ( $\text{Ala} \rightarrow \text{Guest}$ ) replacements that perturb local helical structure.

A special problem potentially compromises accuracy for helical propensities derived from ellipticity data. For a sequence that contains  $n$  alanine residues and a single central guest, the fractional helicity  $\text{FH}$  is a global parameter that equals the average of  $n + 1$  site helicities  $\text{FH}_i$ . We have previously shown that as measures of helix-coil sequence equilibria, the  $\text{FH}$  and any of the  $\text{FH}_i$  are fully equivalent,<sup>17</sup> but practically speaking, the  $\text{FH}_i$  are much more versatile. From a full list of  $\text{FH}_i$  one can exclude the  $\text{FH}_i$  that correspond to sites most susceptible to spurious perturbations, and as shown in the main text, these include sites within end regions as well as sites locally N-terminal to the guest. For a given peptide, a single  $[\theta]_{222}$  is measurable, and it yields only one  $\text{FH}$  value.

A structure- and solvation-induced ellipticity perturbation is clearly embodied in the empirically characterized parameter  $X$  that appears in Equation (2), which is universally used to assign a length-dependence to  $[\theta]_{222,H,n,T}$  from the length-independent core ellipticity  $[\theta]_{222,H,\infty,T}$ . Since  $X$  invariably has a positive value, inspection of Equation (2) shows that a residue at or near an N- or C-terminus must contributes less to  $[\theta]_{222,H,n,T}$  than a core residue.<sup>18</sup>

We have clarified these issues experimentally.<sup>11</sup> For a tailored length series,  $10 \leq n \leq 23$ , of spaced, solubilized polyalanines with exceptional helicities, the  $^1\text{H}$  and  $^{13}\text{C}$  NMR chemical shifts of the helical backbone residues of the two sets of four N- and C-terminal residues are strongly site-dependent, but backbone shifts for the remaining ( $n - 8$ ) core residues have fixed values, independent of site or length  $n$ , and their  $\text{FH}$  values<sup>19</sup> exceed 0.99.

$$[\theta]_{\lambda,H,n,T} = ([\theta]_{\lambda,H,\text{core,Molar}} + [\theta]_{\lambda,H,\text{caps,Molar}})/n = ([\theta]_{\lambda,H,\infty,T}(n - k) + [\theta]_{\lambda,H,\infty,T}(k - X))/n \quad (2a)$$

$$[\theta]_{222,H,\text{caps},T}/[\theta]_{222,H,\infty,T} = (k - X)/k \quad (3)$$

It is conceptually useful to define a new parameter  $k$  as the number of non-core residues within a helical peptide, incorporating it into Equation (2a). (Inspection shows this to be a full equivalent of Equation (2).) For our polyalanine series,  $k$  equals 8. For each series member, the intensity of  $[\theta]_{\lambda,\text{Exper},n,T}$  was measured and expressed in molar units. Their length regressions proved to be strictly linear at all wavelengths, within measurement error, the resulting  $\lambda$ -dependent slopes equal the core per-residue molar ellipticities  $[\theta]_{\lambda,H,\infty,T}$ , and multiplication by the core length ( $n - k$ ) yields molar ellipticities that correspond to the first term of Equation (2a). The second term is  $[\theta]_{\lambda,H,\infty,T}(k - X)$ , which equals  $[\theta]_{\lambda,H,\text{caps,Molar}} = k [\theta]_{\lambda,H,\text{caps}}$ . This is defined experimentally as the intercepts of the

regression. If one divides the value of the intercept at 222 nm by  $k$  and regroups terms, Equation (3) results.

This equation expresses the relative decrease of per-residue ellipticity within non-core regions as a simple function of  $X$  and  $k$ . From three assigned  $X$  values,<sup>5,11,20</sup> we calculate the range at 2 °C for  $[\theta]_{222,H,caps,T}/[\theta]_{222,H,\infty,T}$  as 0.7 to 0.3. Expressed as a penalty percentage, it corresponds to the decrease in  $[\theta]_{222}$  intensity that results if one imagines that one completely helical alanine from the core is transferred to an average site within the end regions. This decrease lies between 30 and 70 % of the core value; it is strongly sensitive to cap structure.<sup>21</sup>

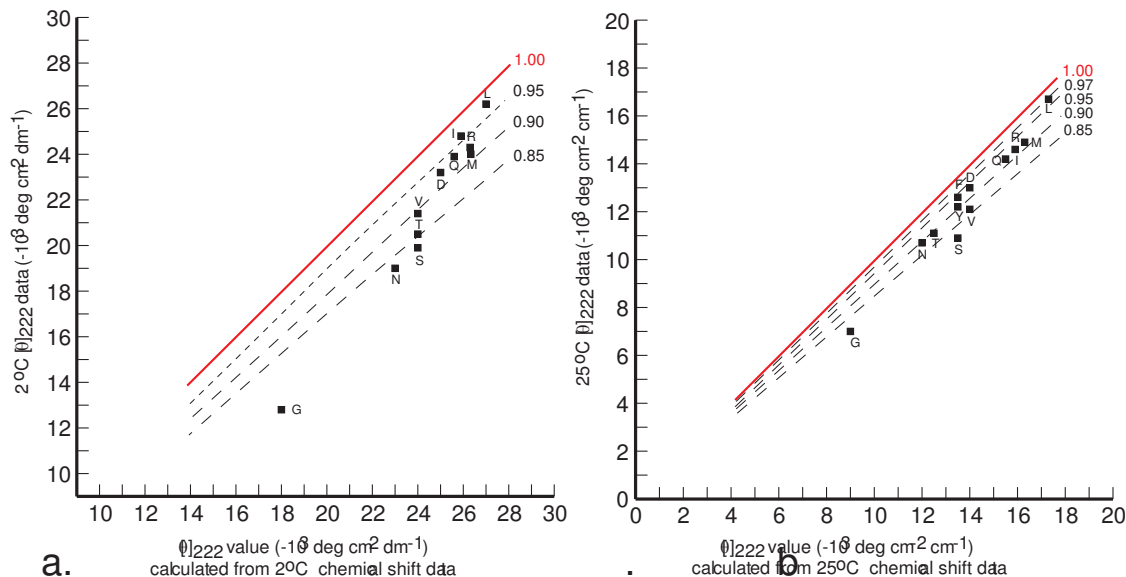


**Figure 1** Value axis squares show experimental values of  $[\theta]_{222,\text{Exper},n,T}$  for mutants  ${}^t\text{L-Ala}_9\text{Xxx}$   $\text{Ala}_9-{}^t\text{L}$  at 2 °C (a) and 25 °C (b). These are plotted parametrically vs.  $[\theta]_{222,n,T}$  values that are Lifson-Roig calculated from relative helical propensities  $w_{\text{Xxx}}/w_{\text{Ala}}$  assigned in the accompanying report from  $^{13}\text{C}=\text{O}$  chemical shifts. The dotted lines in each graph correspond to  $[\theta]_{222,n,T}$  values from a series of calculations using the helical propensity as an independent variable with the range 0.05 to 1.0; for the series, the value of  $[\theta]_{222,H,\infty,T}$  (Equation 2) was multiplied by an attenuating factor within the range 0.97 to 0.85. The red lines show correlations for identical  $w_{\text{Xxx}}/w_{\text{Ala}}$  sets.

What fractional reductions in the value of  $[\theta]_{222,H,\infty,T}$  would be required to generate consistent  $w_{\text{Xxx}}/w_{\text{Ala}}$  sets from both shift and ellipticity data of Figure 5 of the main text? Figure 1 addresses this question. The vertical displacements of the black squares correspond to the  $[\theta]_{222,\text{Exper},n,T}$  data measured at 2 °C and 25 °C for guests Xxx that yield deviant  $w_{\text{Xxx}}/w_{\text{Ala}}$  values. The horizontal

displacements of the squares correspond to  $[\theta]_{222}$  values modeled from propensities assigned from  $^{13}\text{C}=\text{O}$  chemical shift data, as described in the accompanying text, using the host-derived value of  $[\theta]_{222,\text{H},\infty,T}$ . The dotted black lines show modeled values of  $[\theta]_{222}$  calculated from  $[\theta]_{222,\text{H},\infty,T}$ , attenuated by successive factors 0.97, 0.95, 0.90, or 0.85. Inspection shows that with the exception of  $\text{Xxx} = \text{Gly}$ , all ellipticity data can be modeled attenuations within this plausible range. The glycine result deserves comment. Previously reported relative helical propensities for glycine span a fifteen-fold range, and assignments from ellipticity data cluster at the lower end.<sup>22</sup> The Ramachandran permissiveness of a Gly residue strongly suggests that, within a peptide sequence, glycine may be uniquely tolerant of  $\text{3}_{10}$  structure, implying that the appropriate values of  $[\theta]_{222,\text{H},\infty,T}$  for helicity data of glycine mutants must be lower than normal, with a corresponding underestimation of the glycine propensity.<sup>23</sup>

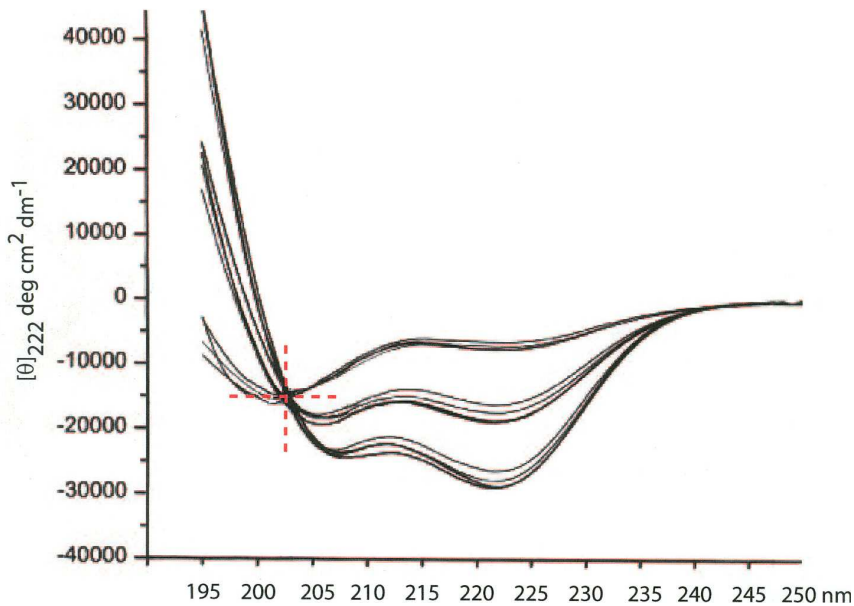


**Figure 2** CD spectra, 190 to 250 nm, at 2, 25, and 60 °C, for the host peptide  ${}^t\text{L-Ala}_{19}{}^t\text{L}$  and for mutants  ${}^t\text{L-Ala}_9\text{XxxAla}_9{}^t\text{L}$ ,  $\text{Xxx} \equiv \text{Nle}$  (norleucine),  $\text{Nva}$  (norvaline), and  $\text{Abu}$  ( $\alpha$ -aminobutyric acid). A well-defined isodichroic point is evident at 202.5 °C with  $[\theta]_{2025,\text{Exper}} = (-15 \pm 1) \times 10^3 \text{ deg cm}^2 \text{ dm}^{-1}$ , consistent with values reported by Holtzer and Holtzer.<sup>2</sup> The two error assignments lie within precision limits.

An independent test for accuracy examines mutant ellipticities measured at 203 nm. The guest-dependent, corrected values  $[\theta]_{222,\text{H},\infty,T}$  that appear in Figure 1 were assigned under the assumption that a wrong choice for this parameter is wholly responsible for the deviations that appear within

Figure 5 of the main text. If this assumption is correct, corresponding guest-dependent deviations should appear if one compares mutant values for  $[\theta]_{203}$ . (The data points of Figure 1 show only the deviant values; no deviations were detected for mutants derived from the non-natural residues Nva and Nle, which bear straight-chain alkyl side chains.) Figure 2 shows superimposed CD spectra measured at 2, 25, and 60 °C for the host peptide  ${}^t\text{L-Ala}_9\text{XxxAla}_9{}^t\text{L}$ , Xxx ≡ Ala for a homologous series of three mutants containing site 10 Abu,<sup>24</sup> Nva, or Nle residues. The twelve CD spectra of Figure 2 exhibit a well-defined isodichroic point at 202.5 nm, with an ellipticity intensity of -15  $\times 10^3$  deg cm<sup>2</sup> dm<sup>-1</sup>, fully consistent with an authoritative literature assignment.<sup>2</sup>

A different picture results if includes in Figure 2 the 2, 25, and 60 °C CD spectra of mutants derived from guests Val, Ile, Met, and Phe. The limits of curve intersections broaden to a wavelength range of 201 to 205 nm, and at 202.5 nm, the error in the ellipticity increases to  $\pm 3 \times 10^3$  deg cm<sup>2</sup> dm<sup>-1</sup>, corresponding to a  $\pm 20$  % relative error, which lies outside data precision limits. A plot of 2, 25, and 60 °C CD spectra of mutants derived from guests Gln, Asn, Ser, Met, Thr, Tyr, Asp, and Glu yields curve intersections that expand to a wavelength range of 200 to 209 nm, and at 202.5 nm, the error in the ellipticity increased to  $\pm 5 \times 10^3$  deg cm<sup>2</sup> dm<sup>-1</sup>, corresponding to a  $\pm 33$  % relative error. These findings definitively validate our conclusion that guest-induced ellipticity perturbations are large enough to explain the accuracies seen in Figure 1. For a majority of the natural amino acid residues, we have proved that CD measurements are unsuitable tools for assigning primary values for host-guest derived helical propensities.

Useful supporting information is also provided by comparisons with double mutant sets as seen in the following table.

**Table I0.** Correlations Between Paired  $w_{Xxx}/w_{Ala}$  Sets.  $Xxx = A, L, M, I, Q, V, F, Y, S, N, T, G$

Set A:  $w_{Xxx}/w_{Ala}$  Assigned from  $^{13}C=O$  Chemical Shifts at Site 14 of Mutants **1**. Set B:  $w_{Xxx}/w_{Ala}$  Assigned from  $[\theta]_{222}$  Values of Mutants **2**. Set C:  $w_{Xxx}/w_{Ala}$  Assigned from  $[\theta]_{222}$  Values of Mutant **2** analogs that contain Two  $Xxx$  guests at Sites 10 & 11.

T, °C	Paired Sets	Slope	Intercept	Fit (SD)	CC	Mean Δ %
2	A - B	1.01	- 0.15	0.08	0.95	+ 41
2	A - C	0.99	- 0.11	0.06	0.97	+ 30
2	C - B	0.95	+ 0.05	0.03	0.99	+ 11
25	A - B	0.96	- 0.09	0.06	0.97	+ 25
25	A - C	0.83	+ 0.01	0.07	0.95	+ 11
25	C - B	0.87	+ 0.08	0.03	0.99	+ 14
60	A - B	0.99	+ 0.06	0.08	0.89	- 8
60	A - C	0.81	+ 0.18	0.04	0.96	- 8
60	C - B	0.64	+ 0.27	0.07	0.84	+ 0.6

## **V. References**

- 
- (1) Yang, J. T.; Wu, C.-S. C.; Martinez, H. M. *Methods Enzymol.* **1986**, *130*, 208—269.
- (2) Holtzer, M. E.; Holtzer, A. *Biopolymers* **1992**, *32*, 1675—1677.
- (3) Wallimann, P., Kennedy, R. J., Miller, J. S., Shalongo, W., Kemp, D. S. *J. Am. Chem. Soc.* **2002**, *125*, 1203—1220.
- (4) Lyu, P. C.; Liff, M. I.; Marky, L. A.; Kallenbach, N. R. *Science* **1990**, *250*, 669—673.
- (5) Job, G. E.; Kennedy, R. S.; Heitmann, B.; Miller, J. S.; Walker, S. M.; Kemp, D. S. *J. Am. Chem. Soc.* **2006**, *128*, 8227—8233.
- (6) Luo, P.; Baldwin, *Biochemistry* **1997**, *36*, 8422—8421.
- (7) Besley, N. A.; Hirst, J. D. *J. Am. Chem. Soc.* **1999**, *121*, 9636—9644.
- (8) Mahadevan, J.; Lee, K.-H.; Kuczera, K. *J. Phys. Chem. B* **2001**, *105*, 1863—1976.
- (9) Woody, R.W.; Sreerama,N. *J. Chem. Phys.* **1999**, *111*, 2844—2845. Manning, M. C.; Woody, R.W. *Biopolymers* **1991**, *31*, 569—586.
- (10) Barlow, D. J.; Thornton, J. M. *J. Mol. Biol.* **1988**, *201*, 601—619.
- (11) Heitmann, B.; Job, G. E.; Kennedy, R. S.; Miller, J. S.; Walker, S. M.; Kemp, D. S. *J. Am. Chem. Soc.* **2005**, *127*, 1690—1704.
- (12) Marshall, C. B., Chakrabartty, A., Davies, P. L. *J. Biol. Chem.* **2005**, *280*, 17920—17929.
- (13) Creighton, T. R. “Proteins: Structure and Molecular Properties”, W. H. Freeman and Co., New York, 1983, p 171.
- (14) Bolin, K. A.; Millhauser, G. L. *Acc. Chem. Res.* **1999**, *32*, 1027—1033.
- (15) (a) Millhauser, G. L.; Stenland, C. J.; Hansen, P.; Bolin, K. A.; van de Ven, F. J. M. *J. Mol. Biol.* **1997**, *267*, 963—974; (b) Long, H. W.; Tycko, R. *J. Am. Chem. Soc.* **1998**, *120*, 7039—7048.
- (16) Toniolo, C.; Polese, A.; Formaggio, F.; Crisma, M.; Kamphuis, J.; *J. Am. Chem. Soc.* **1996**, *118*, 2744—2745.
- (17) Nasr, K. A.; Schubert, C. R.; Török, M.; Kennedy, R. J.; Kemp, D. S. *Biopolymers* **2009**, *91*, 311—320.
- (18) A rigorous distinction between core and ends is justified by the rigid cylindrical structure of a peptide helix. Since for an unaggregated homopeptide sequence of sufficient length, energy perturbations are plausibly all local, and a core must exist in which all residues have the same structure, helix-coil energetics, and per-residue ellipticities. This convergence defines  $[\theta]_{\lambda, H, \alpha, T}$ .
- (19) Assigned from NH → ND kinetics at 2 °C.<sup>11</sup>

- 
- (20) Walker, S. M; Kemp, D. S. unpublished observations.
- (21) For the cap-stabilized polyalanines of reference 11,  $X = 2.5$ ; for the peptides **1**, which contain bulky, hydrophobic 'L spacing regions,  $X = 6$  to  $7$ , and  $X = 4$  to  $5$  for corresponding peptides containing alanine and D-alanine spacers, Kennedy, R. S.; Miller, J. S.; Walker, S. M.; Kemp, D. S. *J. Am. Chem. Soc.* **2005**, *127*, 16961—16968.
- (22) Luo, P.; Baldwin, R. L.; *Proc, Natl. Acad. Sci. USA* **1999**, *96*, 4930—4935.
- (23) Lee, J.; Kemp, D. S. unpublished observations.
- (24) The required synthetic facilities and personnel were no longer available to us for synthesis of a mutant **1** that contains  $^{13}\text{C}=\text{O}$  reporters and a site 10 Abu =  $\alpha$ -aminobutyric acid guest.